

On Transpositional Topology

Rasmus Joergensen, Christian Waldvogel

October 1, 2021

Abstract

We propose a framework for the intuitive generation of an infinite set of chiral, highly symmetric and regular tessellations of surfaces. Our method lets us create and describe abstract polytopes based on combinatorial polygons and simple, generative rules. Represented as graphs, these polytopes can be embedded in geometric spaces using well known force directed algorithms.

More specifically, by introducing the notion of fixed and transpositional edge colours, we show how tilings of the hyperbolic plane, the euclidean plane and the sphere arise naturally as realisations of merely additive colour matching rules. Furthermore, we grow tilings of more complex genus " ≥ 1 "-surfaces like the Klein quartic or the mutetrahedron by naturally extending our generative rules with cross-tile, cyclical walks encoded using colour sequences.

In order to systematically explore the space of possible tessellations, we develop a notation for the base tile colourings as well as the cyclical walks and provide a list of all possible tiles with up to 13 edges.

The software implementation of our framework (**grasp**) based on widely used libraries and algorithms[5][7][4][6] has helped us generate rich empirical evidence for its value in understanding the structure of well known discrete surfaces as well as creating, what we believe to be previously unknown regular tessellations of others.

The stability of the geometric embeddings produced by introducing simple edge based metrics hints at the truly astonishing symmetric properties of many of the combinatorial surfaces emerging from the interplay of the different components in the proposed framework.

1 Introduction

Let us begin with a few words on the chosen structure of this document. Since we follow a generative and exploratory approach to surface generation, which we would like to make as widely accessible as possible, we have chosen to separate its presentation into three parts. The first part will be a more intuitive account of the our generative process, which aims to give the reader a coherent account of the present results. The second part contains more detailed descriptions and definitions of the underlying mathematical structures, while the appendix lists further results and tables.

The tilings we describe in this paper were produced using the software **grasp**¹ and their embedded edge-coloured graphs have been made publicly available for download, verification and contemplation².

The research presented here took its origin in the exploration of heptagonal tilings as a means to find hitherto unknown minimal surfaces. So in contrast to studying the projection of a heptagonal tiling onto known continuous minimal surfaces, we pursued a generative bottom-up approach, using predefined rules to add heptagonal tiles to one another. Initial experiments were based on physical models (Figure 1) consisting of regular heptagons made out of paper, which, when glued together three to the vertex, warp and bend.

The working hypothesis was that minimal surfaces could be created by looping the thus created structure rather than letting the surface play out to get more and more crumbled up at the edges like the leaf of a lettuce.

Several well known surfaces exists that can be tiled by heptagons, for example the hyperbolic plane or the Klein Quartic as well as minimal surfaces like for example the Schwarz d- and p-surface.

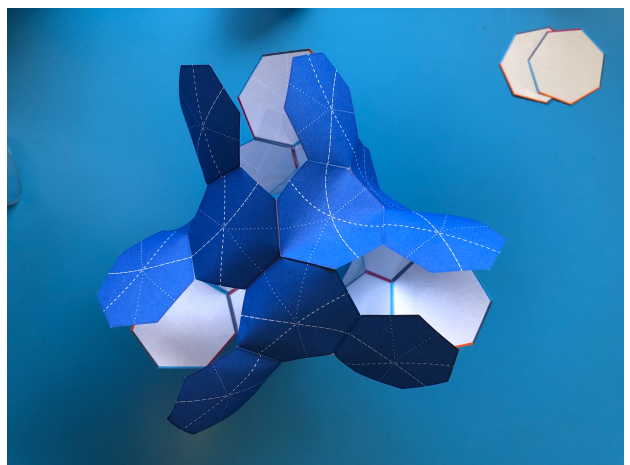


Figure 1: Physical Models

In order to be able to classify and systematically explore the seemingly endless space of possibilities for the loops described above, rule sets were sought that could guide the generation of these surfaces and indicate hitherto unexplored paths. The first major

¹If you are interested in getting access to the source code of grasp, please contact us

²<https://transpositional.org/>

breakthrough in that direction was the discovery of an heptagon edge-colouring that restricts how each heptagon may be glued to its equally coloured neighbours, but still allows for a $\{7,3\}$ tiling of the hyperbolic plane. The colouring constituted a tighter definition of the tile symmetries at play by imposing a secondary structure to the ordinarily homogeneous edges of the heptagons (figure 2).

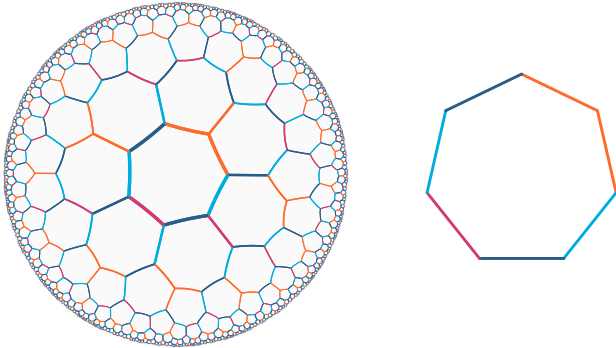


Figure 2: Coloured Hyperbolic Plane and Tile

Using this colouring and combining multiple tiles to repeatable modules, physical models were built that replicated the structure of well known surfaces like the Schwarz d- and p-surface, but it soon became clear that the vast space of possible surfaces could only be explored efficiently with the help of computers. With the introduction of software to the surface generation a stronger formalisation of the related problems took place. Edge-coloured graphs were for example used as a means to describe tiles and generated structures and the need to symbolically describe the act of gluing sparked reflections on the implicit algorithmic assumptions present when working with paper.

Despite or exactly because of the incredible richness of our first results, the answering of questions pertaining the uniqueness of the heptagon tilings gained increasing importance.

Is the intricacy found in the created structures an intrinsic property of the coloured heptagon or can similar structures also be constructed using colourings of other n-gons? If the heptagon is unique, what constitutes its differentiating properties? Its colouring, its geometry or a combination of both?

To answer these questions, it became necessary to distil the colour based rules down to their essence, to extend the scope of possible tiles to encompass any polygon and to abstract away the notion of geometry all together. While, as we learned in a late state of our research, the resulting purely combinatorial approach is tightly related to abstract polytopes and combinatorial maps, we find the notion of directed multigraphs in the form of Half-Edge-Datastructures[1] better suited to intuitively convey the encoding of the specific combinatorial properties developed here. We will therefore describe our framework using mainly graph theoretical definitions and

save the evident relationships with these fields for a later paper.

2 Framework

We will start our exposition by defining the basic building blocks used in our framework, the colours. Then we will proceed to show how multiple colours are combined to form tiles and how multiple tiles come together to form combinatorial tilings that can be embedded as surfaces in more intuitively accessible spaces like E^2 , H^2 or E^3 .

2.1 Tiles and Colours

We start our process by defining a colour cycle. For every element of the cycle, we choose from two types of colors.

- **fixed colors** Every colour of type fixed colour must only occur once in a cycle
- **transpositional colors** Every colour of type transpositional colour must occur exactly twice in a cycle

We define cycles consisting of only fixed colors, only transpositional colours or of both as n-colourings, where n denotes the number of elements in the cycle. n-Colourings are the basis of our tiles.

To form a tile, we create a directed cycle graph or directed n-gon similar to its geometrical counterpart the polygon, consisting of n vertices and n directed edges and bijectively as well as sequentially map the elements of the n-colouring to the edges of the graph along the direction of the edges. See figure 3a.

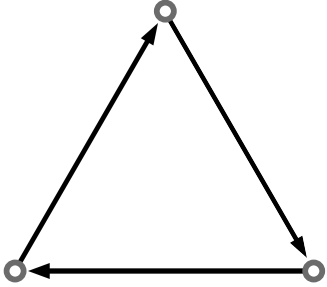
The number of differently coloured tiles with n edges thus becomes a matter of possible permutations of fixed and transpositional colours for the n elements of an n-colouring. Simple examples of 3-colourings of a tile can be seen in figure 3.

As a matter of fact, the two displayed colourings are the only possible colourings of the 3-gon. With three edges at our disposition, we can only either label all edges with a fixed color or we can choose to label two of the three edges with a transpositional color, which leaves us with no choice but to assign a fixed color to the remaining edge.

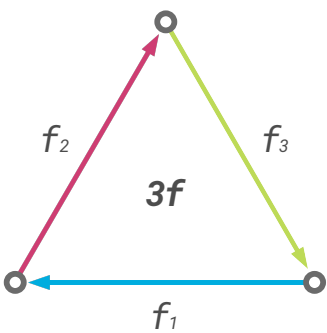
2.1.1 Signatures and Labeling

In order to be able to systematically and unequivocally identify any possible n-colouring permutation, a signature was developed that reflects the unique structure of any n-colouring and enables us to consistently address vertices, edges and their relative position within n-coloured tiles. Subsequently as a basis for further inquiry an index of all possible n-colourings up to $n = 13$ was computed. See section 4.6.

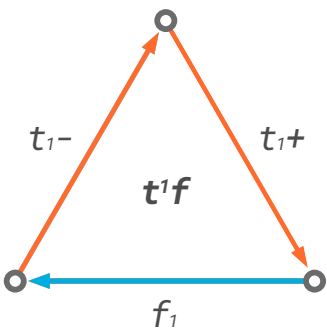
While, as can be shown, it is simple to create an n-colouring based on the signature, developing such a



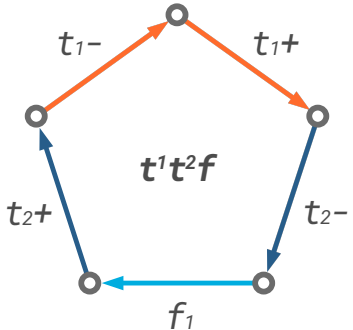
(a) Directed Cycle



(b) 3-colouring with three Fixed Colours



(c) 3-colouring with one Transpositional Colour and one Fixed Colour



(d) 5-colouring with two Transpositional Colours and one Fixed Colour

Figure 3: Colouring of Tiles

unique consistent notation for any n -colouring is less trivial due to the cyclical structure of the colourings. For a more formal treatment of this problem as well as for the notion of n -colourings, see section 4.1.1.

Here, we will limit ourselves to a short guide of how to read the notation, since it will come in handy throughout the further elaborations.

A signature consists of a series of symbols f and t^d , denoting the sequence of occurrences of the two types of colours in a n -colouring. With t^d we denote the first occurrence of a transpositional colour and its distance d to its second occurrence along the cycle. $d = 1$ indicates that the next element in the cycle would be of the same transpositional colour, while $d = 2$ would indicate that another color is located between the two occurrences of the a transpositional color etc. With f we denote the occurrence of a fixed colour. Evidently the distance between a fixed colour and itself along the cycle will always be n , since it by definition may only occur once. We can thus safely omit the distance for brevity's sake.

As a last component of our signatures we introduce multipliers to enable us to further compactify the notation. Multipliers indicate multiple uninterrupted occurrences of fixed colours or multiple uninterrupted occurrences of equidistant transpositional colours within the cycle.

As mentioned above, only the first occurrence of a specific transpositional colour is marked by a t^d . The second occurrence of the same transpositional colour is not marked but implicitly indicated by d . Obviously a notion of first and second is not easy to come by in a cycle and necessitates the introduction of a uniquely defined reference element any other element can be related to. How this is accomplished can be learned in section 4.1.1.

signature	cycle	
$3f$	(f, f, f)	Defines a 3-gon with 3 edges of fixed color. Uses the multiplier 3 to indicate the repetition of the 3 consecutive fixed colours. See figure 3b.
t^1f	(t_1^-, t_1^+, f)	Defines a 3-gon with 2 edges of transpositional colour following each other and 1 fixed colour edge. See figure 3c.
t^1t^2f	$(t_1^-, t_1^+, t_2^-, f, t_2^+)$	Defines a 5-gon with 2 consecutive edges of the same transpositional colour followed by another transpositional color, that encloses a fixed color. See figure 3d.

Table 1: n -Colouring Notation Examples

Having a reference element will not only allow us to define a n -colouring's unique signature but also pro-

vides us with the desired means to name its colors and to index the vertices of its derived tile in a consistent manner.

Starting with the reference element of the n-colouring and proceeding along the cycle, we name the fixed and transpositional colors with f_p and t_q respectively where subscripts $p \in \mathbb{N}$ and $q \in \mathbb{N}$ number the colors consecutively and separately by type, starting at $p, q = 1$. It is important to note that both instances of a transpositional color will be numbered with the q of its first occurrence. To be able to address them individually, the first instance will be signed with a - and the second with a +. See table 1 for examples.

The vertices of the coloured base tile $V = \{v_1, \dots, v_n\}$ are numbered in such a way that v_1 will be the source vertex of the edge labelled with the reference element of the n-colouring, v_2 the source of the second edge in the cycle and so on.

A short note on the use of colour in diagrams. A consistent colour coding has been used to facilitate the readability of diagrams. Tile edges will be coloured based on their type and index. See section 4.8.

2.2 Glueing Rules

After having described how we generate tiles from colour cycles, we turn to how these basic building blocks are combined. An intuitive way of thinking about the combination of tiles, is that we glue tiles together at the end-vertices of matching edges.

The overall result of one or several gluing operations, we call a **tilegraph**. In the context of glueing operations between tiles, we will refer to edges of a single tile as half-edges. Two combined half-edges of two different tiles will be referred to as a full-edge in the tilegraph.

Consequently, tilegraphs can be thought of as directed half-edge multigraphs, made up of their constituting tiles' coloured directed cycles, which share vertices along the glued edges. See also section 4.8.

Our framework governs the glueing process by the following rules.

Colour Rule Glueing of two tiles is only allowed along half-edges of the same fixed colour, or along half-edges of the same transpositional colour but differing signs.

Simplex Rule Only exactly two half-edges can be glued at their end-vertices to form a full-edge of the resulting tilegraph. Edges of tiles, which have already been glued, cannot be glued again.

Self-Connect Rule A tile is not allowed to connect to itself.

Orientation Rule When two half-edges are glued together to form a full-edge in the tilegraph, they must point in the opposite direction and form a cycle in their own right.

Zip-Up Rule If the source and/or target vertices of the glued half-edges are part of further matching half-edges, these must also be glued.

With the following two exceptions:

Subdivision Exception If glueing the matching half-edges would lead to two consecutive full-edges between the same tiles, then glueing is not allowed.

Gyre Exception If glueing the matching half-edges would subceed the lower bound defined for the number of faces that must surround either the source or the target vertex, then glueing is not allowed.

We call this the gyre exception since the lower bound will be defined via the concept of gyres, which we will lay out in section 2.4. Restated using the notion of gyres, the exception is defined in the following way: If the gyre, which a source or target vertex of the glued edges corresponds to, has a gyre multiplier bigger than the default of 1, matching edges can only be glued, iff multiplier times half the unit gyre cardinality is at least equal to the number of tiles, which the end vertex would be part of.

Continuation Rule Any rules above must hold for any further glueings induced by the *zip-up rule*.

To summarize:

- The *colour rule* governs the edge matching process.
- The *simplex rule*, *self-connect rule* and *orientation rule* are in place to ensure that there is a path from the combinatorial structure to a "well" formed oriented surface, without cone points and one edge faces.
- The application of the *orientation rule* will result in chiral abstract polytopes that do not exhibit mirror symmetries along edges as long as the colouring is being considered as part of the combinatorial structure.
- The *continuation rule* and the *zip-up rule* guarantee the application of the previously mentioned rules throughout the tilegraph.

Let us see how the glueing rules are applied to tiles.

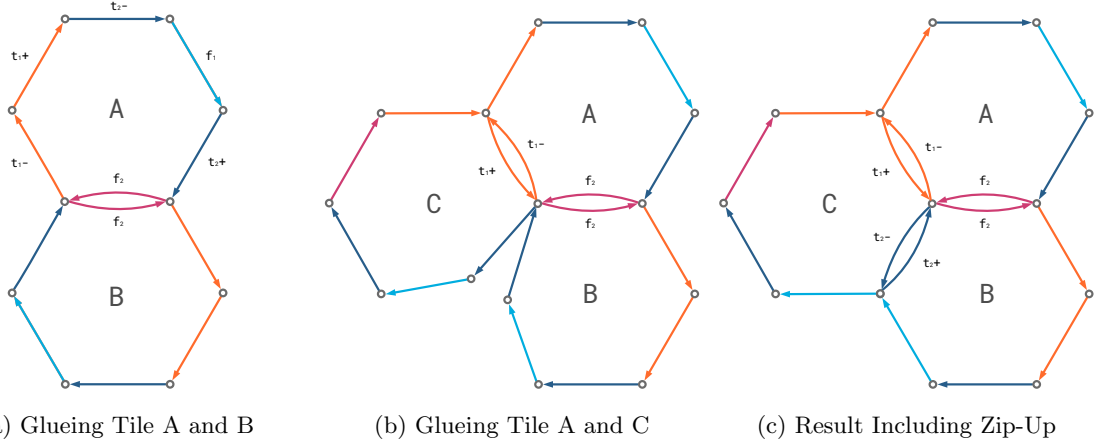


Figure 4: Glueing of Tiles

Example Figure 4 shows a simple example of glueing three t^1t^22f hexagon tiles together.

- Figure 4a shows how first tile A and B are glued together to form a tilegraph by merging the starting vertex of the fixed colour half-edge $f_2(wine)$ of tile A with the end vertex of the $f_2(wine)$ half-edge of tile B and vice versa.
- Figure 4b shows how tile C is added to the tilegraph containing A and B by merging the starting vertex of the transpositional colour half-edge $t_1+(kaki)$ of tile C with the end vertex of transpositional colour $t_1-(kaki)$ of tile A and vice versa. Please notice how $t_2-(navy)$ of tile C and $t_2+(navy)$ of tile B line up and create the necessity for a zip-up.
- Figure 4c shows how the final result of glueing tile A and C including the induced zip-up of C and B.

As a short side note related to the labelling of vertices, in the context of a tilegraph, where vertices are shared between the tiles, it is still possible to label the vertices in the way described under section 2.1.1, but obviously only in relation to a specific tile in the tilegraph.

With the glueing rules in place and an example of how they act on tiles behind us, we are ready to demonstrate the generative power that arises from the introduction of the transpositional colors.

In figure 5 we show how the introduction of transpositional colours acts on a set of six tiles to form a cubical digraph. Imagine starting out with 6 tiles of 4 edges each, coloured in exactly the same order by 4 different fixed colours. We label the tiles A through F and the edges f_1, f_2, f_3, f_4 along the cycle or according to our colour coding definition (see section 4.8) *cyan, wine, lime, jade*.

Now starting with tile A, we add tile B along the edge coloured $f_1(cyan)$ following the glueing rules defined above. We continue by adding C along $f_2(wine)$, D along $f_3(lime)$ and E along $f_4(jade)$. By adding

F along $f_2(wine)$ of E , we complete the composition of the 6 tiles.

The result can be seen in subfigure 5a, which also shows that none of the glueings defined so far would lead to the application of the *zip-up rule*. Take for example the opposing edges between B and E . Since the $f_2(wine)$ coloured edge of B does not match the $f_3(lime)$ coloured edge of E , no zip-up occurs. For this rule to take effect, we would need to add another tile in between B and E , as hinted in the subfigure, for example to $f_2(wine)$ of B , which would automatically lead to a zip-up of the new tile with E .

It can easily be seen that the fixed coloured edges coming together at the vertices in this first example will always be the same, since all edge-colours are represented around any vertex. If we would thus continue to glue tiles to our current tilegraph, the glueing rules would lead to a monotonic expansion of the tilegraph with 4 tiles around every vertex. Such a tilegraph can evidently be regularly embedded into E^2 as a square tiling.

Subfigure 5b shows what would happen if we would replace the $f_3(lime)$ and $f_4(jade)$ edges of all our tiles with another colour *kaki* and still use our glueing rules.

Since the previous $f_4(jade) - f_4(jade)$ and $f_3(lime) - f_3(lime)$ matching edges would now be replaced by *kaki* – *kaki* matching edges all tiles can be left in place. We see though, that a zip-up would occur between B and C .

We could now of course try other variants of *kaki* – *kaki* matchings by rotating the tiles, since the relationship between tiles are now not uniquely determined by the colors. Two tiles could be connected in four ways via *kaki*. Rather than allowing such ambiguous relationships between tiles, we take the final step towards the use of transpositional colours and define *kaki* as $t_1(kaki)$ and thereby sign the two $t_1(kaki)$ edges with – and +.

Since all tiles need to be equally coloured, we take care that the edge following $f_2(wine)$ is marked with a – and the edge preceding $f_1(cyan)$ is marked with a +. When marking the tiles in such a way and keeping

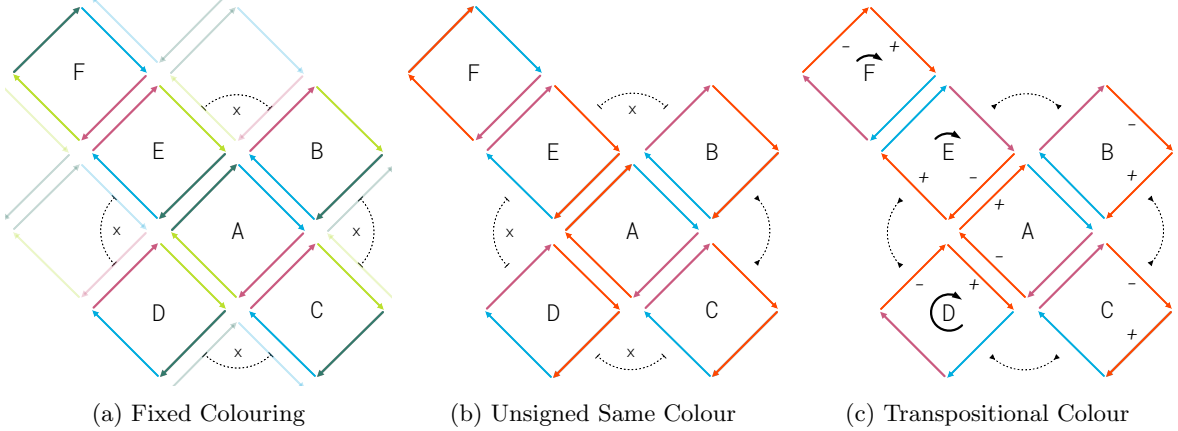


Figure 5: Combinatorial Performance Transpositional Colours

A in place, we will need to rotate D, E, F in order to match the coloured edges up again based on the rule that only transpositional colours of opposite sign can be glued together.

D will need a three-quarter turn clockwise and E and F will need a one quarter turn clockwise for the colours to line up. The effect can be seen in subfigure 5c. What can also be taken from that figure is that the *zip-up rule* would start to take effect. B zips up with E, C, F and the same is true for D . Since edge $f_4(\text{jade})$ of C and edge $f_4(\text{jade})$ of F also match up, the tilegraph can be considered closed. No unglued half-edges exist after zip-up. With 6 tiles, 8 vertices and 24 half-edges (amounting to 12 full-edges), the tilegraph forms a cubical graph.

2.3 Undirected Tilegraphs

As is obvious from the foregoing elaborations on the cubical digraph, the notion of full-edges as a combination of two half-edges can be somewhat confusing when comparing tilegraphs with other well known named graphs or surface structures. To simplify this, we introduce the notion of undirected tilegraphs.

Undirected Tilegraph An undirected tilegraph is constructed from a regular tilegraph by merging all glued directed half-edges to one undirected full-edge and removing the direction of all unglued half-edges.

Merged full-edges will be labelled with the colour name of their constituting half-edges. In the case of transpositional colours the label of the full-edge loses its sign. Undirected half-edges retain their colour label.

2.4 Gyres

In the example above we showed how tilings of surfaces with genus 0 (the square graph and the cubical graph) emerge naturally, merely by applying the glueing rules to the n-coloured tiles. For a more stringent argument of why glueing rules lead to tilegraphs,

which can be interpreted as tilings of topological discs or spheres, see section 2.7.

In order to complete our understanding of the *zip-up rule* and the emergent features of the generated genus 0 surfaces, we will in this section introduce further terminology and tools based on the notion of gyres, which will be elemental to understanding and discussing further more complex examples of tilegraphs. For this purpose we shift our attention from the colour cycles along the edges of tiles to the colour cycles of the edges incident to the vertices in our tilegraphs as governed by the glueing rules. Or more bluntly put, instead of focusing on edge cycles around tiles, we now focus on edge cycles around vertices.

We introduce the following new concepts.³

Gyre We call the subgraph consisting of all edges incident to a vertex of a tilegraph a gyre, provided that all the incident half-edges have been paired to create full-edges. Thus, gyres emerge from the application of the glueing rules. See figure 6.

Pivot The set of vertices of a n-coloured tile, that will, as part of different tiles, meet at the center of a gyre in the tilegraph, we call a pivot. By convention, we address the pivots and gyres in relation to an n-colouring signature's starting colour. Thus the source vertex of the edge coloured by the first colour of the n-colouring will belong to $pivot_1$ at the center of $gyre_1$. The next vertex along the tile cycle that belongs to another pivot and gyre will be part of $pivot_2$ at the center of $gyre_2$ and so forth.

Gyre Order The order of a gyre is established naturally by glueing tiles around a vertex of a n-colouring. Create a tile A based on any n-colouring and choose the vertex v , for which the gyre needs to be determined. To establish a unique direction of the gyre cycle, we now begin by adding the colour of the half-edge a_1 incoming

³For a more formal treatment of the subject see definition 4.4.

to vertex v as the first color. We follow up with what we call a sharing step and add the colour of the half-edge a_2 outgoing from v . As a first glueing step, we combine tile A via half-edge a_2 to tile B via matching half-edge b_1 and append the colour of b_1 to the gyre. The end vertex of b_1 will be part of the pivot at the center of the gyre. We continue adding tiles around v and their corresponding colours to the gyre until zip-up occurs as the last glueing step.

Another way to look at the gyre order, is to see it as the sequence of edge-colours you would encounter, if you walked across the tiles around a pivot, crossing the tile edges incident to the pivot. See figure 6

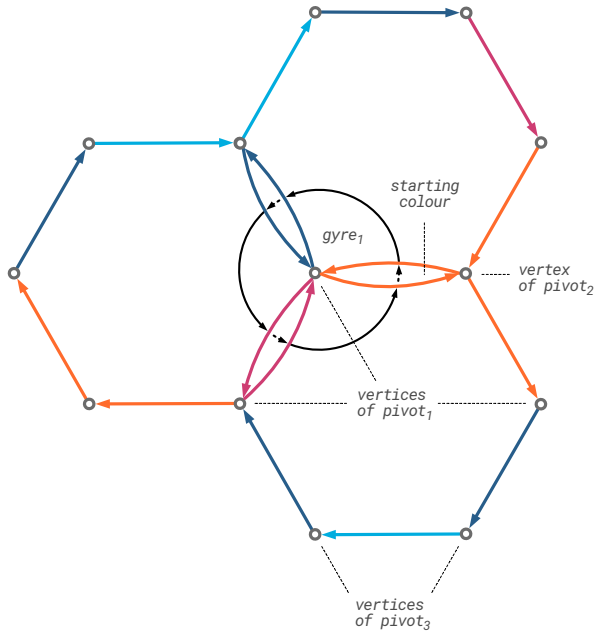


Figure 6: Gyre Walk and Marked Gyre Pivots

Unit Gyre The gyre around a vertex v that would be generated by the glueing rules, if the *self-connect rule* and the exceptions to the *zip-up rule* were ignored or in other words, if we would allow vertices of indegree $\deg^-(v) = 1$ or $\deg^-(v) = 2$.

Gyre Multiplier The gyre multiplier is a natural number $gm \in \mathbb{N}$. It defines how many unit gyres have to be present around its pivot before the *zip-up rule* can be applied. The default gyre multiplier for any gyre is $gm = 1$.

Gyre Degree The number of faces coming together in the vertices belonging to the gyre's pivot. The indegree $\deg^-(v)$ of any vertex v in the tilegraph will be half the cardinality of the corresponding unit gyre $gyre_u(v)$ times its gyre multiplier $gyre_{mult}(v)$ with a lower bound of 3.

$$\deg^-(v) = \max\{3, \frac{|gyre_u(v)|}{2} * gyre_{mult}(v)\}$$

The lower bound of 3 is given by the *self-connect rule* and the *subdivision exception* to the *zip-up rule*.

Monogyre/Polygyre A monogyre is a gyre consisting of only one transpositional color. A polygyre consists of multiple fixed and/or transpositional colors.

Based on these concepts, we can make several observations.

- As we saw when describing the gyre order, any colour in the gyre will be the result of one of two steps: The glueing step and the vertex sharing step. A glueing step will always be followed by a sharing step and vice versa. They alternate. Consequently a colour added to the gyre based on a sharing step will become the source of a glueing step and vice versa.
- The outcome of the sharing step is uniquely defined by the n-colouring, the outcome of the glueing step is made unique by the glueing rules. Since the steps are uniquely defined, any vertex of a tilegraph can only belong to one pivot or be at the center of one gyre.
- Unit Gyre and gyre multiplier are particularly interesting for vertices between two consecutive edges of same transpositional color. Since the unit gyre of any such monogyre would be incident to two tiles only, we can define the number of incident tiles in such vertices to be any number $\mathbb{N} \geq 3$ by means of a gyre multiplier.

Parallels can be drawn between the relationship of gyres and n-colourings within tilegraphs and the representations of combinatorial maps via a vertex centred rotational system or a face centred representation. The main difference being the way half-edges, as used in face centred representations of combinatorial maps, are kept within the vertex centred gyres and do not disappear as they do in rotational systems.

While both vertex-centred and face-centred representations are equally suited to describe general combinatorial maps, defining a tilegraph by face-centred means using n-coloured tiles is much more compact, than describing it by the different gyres it generates. At least as long as we stay within the realm of regular tilegraphs based on one n-colouring only. Nevertheless, gyres and pivots tell us more about how many types of vertex neighbourhoods there are, as well as what degrees vertices in a tilegraph will have. They are invaluable tools in the process of evaluating the feasibility for an n-colouring to generate a certain type of abstract polytope, apeirotope or basis for an embedded surface.

2.4.1 Gyre Graphs

In order to get a better grasp of the pivots and gyres occurring in tilegraphs, the so called gyre graph was

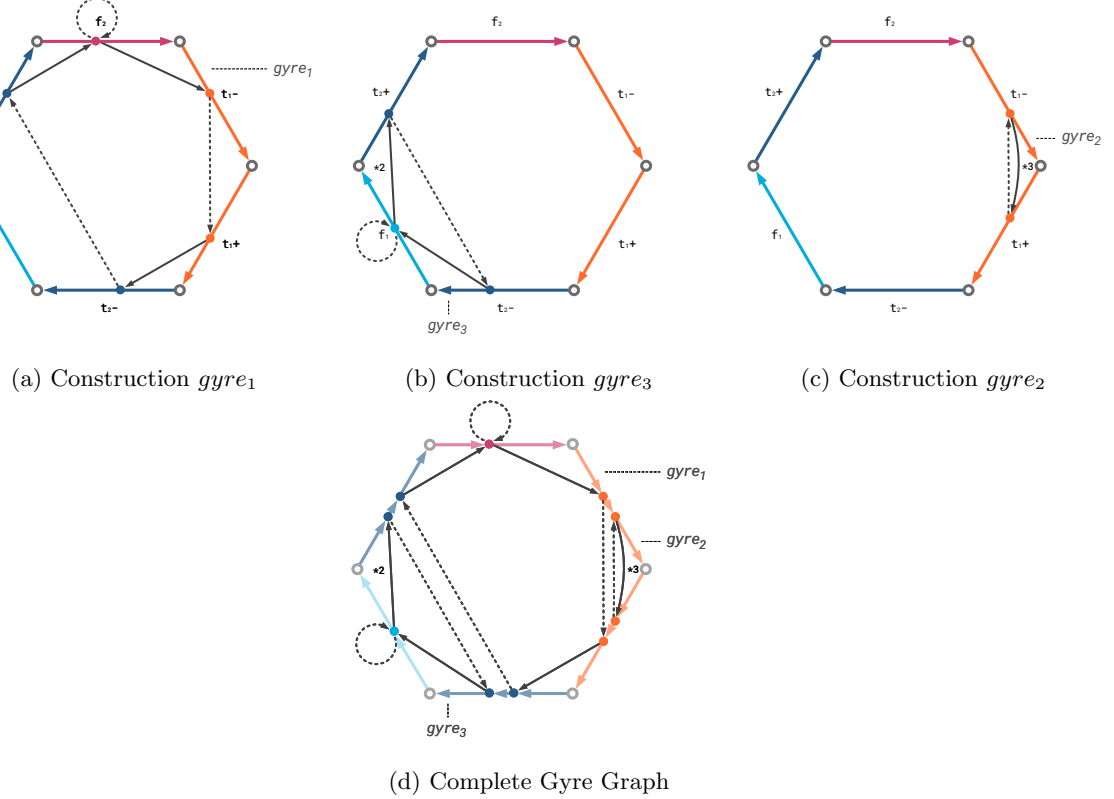


Figure 7: Gyre Graph Construction

developed. A simple instrument that helps to expose the combinatorial structure of n -colourings and maps out resulting gyres and pivots.

Since we know that any edge-colour will end up in a gyre and gyres are per definition dependent on the order of the n -colouring, we start our construction of the gyre graph by drawing the tile of the base n -colouring as an equilateral n -gon. In the example shown in figure 7 we use t^1t^22f . Starting from this graph, we take the following steps to construct the first gyre of the gyre graph.

1. Pick any edge to start with for example $f_2(\text{wine})$. We know that any such coloured edge in a tile-graph would share a vertex with the next edge in the cycle $t_1-(\text{kaki})$, so we draw a new edge in the tile from $f_2(\text{wine})$ to $t_1-(\text{kaki})$.
2. As per our glueing rules $t_1-(\text{kaki})$ will be glued to $t_1+(\text{kaki})$ of a new tile, so we draw a dotted edge from $t_1-(\text{kaki})$ to $t_1+(\text{kaki})$ in our graph.
3. We know that, within this new tile, $t_1+(\text{kaki})$ will share a vertex with $t_2-(\text{navy})$, so we continue with a new edge between these edges in our graph.
4. Continuing this procedure, we find that $t_2-(\text{navy})$ will glue to an edge $t_2+(\text{navy})$ in a new tile, which will at its turn share a vertex with $f_2(\text{wine})$. And $f_2(\text{wine})$ will glue to $f_2(\text{wine})$ of our starting tile, thus we have completed the representation of $gyre_1$.

Again we see the structure of alternating sharing and glueing steps described above. The glueing steps being represented by dotted edges and the sharing steps by solid edges. We find the expected pattern that the fixed colour $f_2(\text{wine})$ has been source and target of glueing steps as well as sharing steps, while the transpositional colours can still be part of further gyres. Therefore, let us have a look at how the other gyres would be formed.

1. We start off with $t_2-(\text{navy})$, that was already added to $gyre_1$ due to a glueing step and pick the next edge it would share a vertex with within the same tile, $f_1(\text{cyan})$. Hence, we draw a solid edge from $t_2-(\text{navy})$ to $f_1(\text{cyan})$.
2. $f_1(\text{cyan})$ will connect to $f_1(\text{cyan})$ of an adjacent tile and thus we connect it to itself.
3. $f_1(\text{cyan})$ shares a vertex with $t_2+(\text{navy})$, so we connect these two.
4. Now $t_2+(\text{navy})$ matches $t_2-(\text{navy})$, which is the edge we started with in the gyre and we could close our cycle, were it not for the *zip-up rule* that states that two adjacent tiles may not have two consecutive full-edges in common. This would be the case if we close, because we have only taken two glueing steps and thus switched tile twice, between $f_1(\text{cyan})$ and $f_1(\text{cyan})$ and between $t_2+(\text{navy})$ and $t_2-(\text{navy})$. So we must continue to walk the cycle and thus add two more tiles adjacent to the pivot to comply with the

glueing rules. Consequently, the resulting $gyre_3$ consists of two repetitions of the same colour sequence. We denote this in the gyre graph by a $*2$ rather than actually drawing the repeating edges.

To complete our gyre graph example, we still need to add one more gyre. We have not yet considered the sharing step of $t_{1-}(kaki)$.

1. We start off with $t_{1-}(kaki)$ that was also already added to $gyre_1$ due to a glueing step and pick the next edge within the same tile that it would share a vertex with, which is $t_{1+}(kaki)$. Hence, we draw an edge from $t_{1-}(kaki)$ to $t_{1+}(kaki)$.
2. The special case of two consecutive edges of the same transpositional colour in an n-colouring becomes evident, since $t_{1+}(kaki)$ immediately matches $t_{1-}(kaki)$ and were it not for the *self-connect rule*, the gyre would be complete and the vertex incident to the transpositional colour edges would become a cone point. Thus similar to the case in $gyre_3$ we need to add another sequence to the gyre, which in this case consists of $t_{1-}(kaki)$ and $t_{1+}(kaki)$.
3. Now we have stepped through two glueings and again the gyre cannot close up, due to the exception *subdivision exception* to the *zip-up rule* and yet another sequence needs to be added before the *zip-up rule* will take effect. We end up with three times the same colour sequence unless a gyre multiplier bigger than 3 was defined, in which case the sequence adding would continue until the desired number of unit gyres was reached. We denote the result with a $*3$ or $*td$ respectively in the gyre graph.

Figure 7d shows the final gyre graph with the three different gyres. Two of them polygyres containing multiple colours and one a monogyre. To see which vertices belong to the pivot of any gyre, follow the arrows of the gyre. Any vertex "cut" off by a solid arrow sharing action will be a pivot vertex of the gyre. To get the incoming degree of any vertex in a final tilegraph, count the number of solid arrows in the corresponding gyre and multiply by the gyre multiplier. The incoming degree also directly corresponds to the number of incident tiles in the vertices.

With the gyre graph construction explained, it is now simple to visually grasp the two following observations about gyres.

- Due to the *orientation rule*, the end vertex and start vertex of any fixed colour will be mapped to each other. Both vertices will belong to the same pivot and be at the center of the same gyre.

It follows that any fixed colour can only be part of one gyre as well. This also means that any n-colouring consisting of only fixed colours will have only one gyre and one pivot and all vertices of the resulting tilegraph will have incoming degree $\deg^-(n)$. See figure 8a.

- The end and start vertices of a signed transpositional colour can be part of two pivots, since they do not directly map to each other. Examples can be found though, where both vertices belong to the same pivot and thus the transpositional colours would only be part of one gyre. See figure 8b

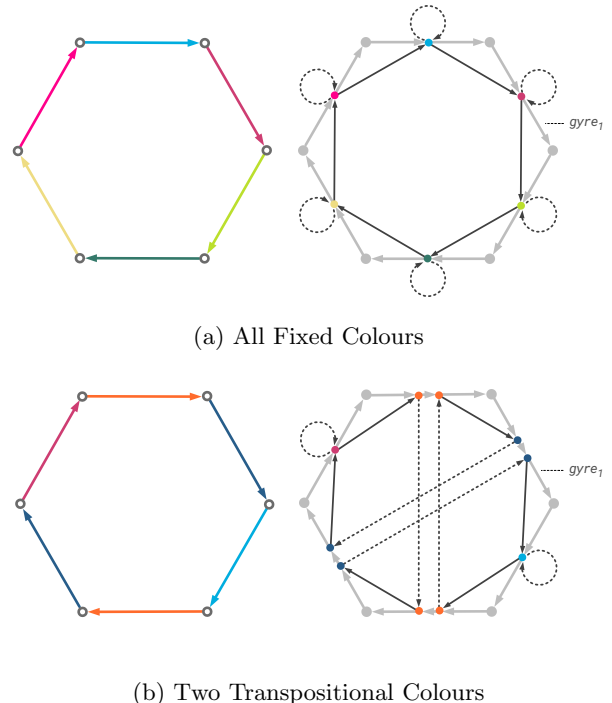


Figure 8: One Gyre Examples

For reference purposes, the number of incident tiles at any n-colouring vertex has been computed and added to the n-colouring tables in section 4.6 of the appendix. The data can be found in the column *Tile-Vertex Incidence* as an ordered sequence, starting with the number of tiles at the vertex between the first two colours of the n-colouring and continuing along the directed cycle of colours. In the same table, the number of different gyres is also provided in *Gyre Count*.

This almost concludes our development of the necessary tools to construct abstract surfaces based on n-colourings, at least in regards to surfaces of genus 0. What remains to be defined is the notion of growth.

2.5 Growth

As mentioned in the introduction, our framework develops surfaces bottom up. In a certain sense they can be thought of as being grown. For the examples explored here, we have decided on the following easily understandable and implementable growth strategy.

Growth Strategy Starting from a single n-coloured tile, every growth iteration realizes the gyres around all vertices along the boundary (or boundaries) of the tilegraph by adding tiles one

by one along the gyre and applying the glueing rules for every tile addition. Thus, after a growth iteration all boundary vertices resulting from the previous iteration will become inner vertices, all half-edges left open by the previous iteration will be paired with half-edges of added tiles and all added tiles will be glued to each other where possible due to the *zip-up rule*.

We explicitly do not impose any restriction on the initial vertex chosen for the realization of the gyres, but once chosen, we proceed vertex by vertex along the boundary's direction.

Other growth strategies would of course be conceivable, sometimes leading to results possibly more in line with desired objectives, similar to the way the "decapod"-seed is used in Penrose tilings to attain a regulated growth continuity[9]. Using the growth strategy above, we could for example generate a 6-gon tilegraph of indegree 4 using $t^2t^3t^2$, which can be regularly mapped to the hyperbolic plane. If we do not start with a single tile though, but with a ring of 6 tiles always connected via the t_1 colour, the ring will never close and growing the tilegraph iteratively along the boundaries will yield a tilegraph with one neck. See section 4.5.2.

What needs to be considered as well though is that a badly chosen strategy can also lead to premature dead ends. This is for example the case in the example under section 4.5.1 of the appendix, where using the tilegraph prior to the last step as a seed, would not admit even one growth iteration, since the *continuation rule* would not hold., as is shown.

How seeds and growth strategies impact the created tilegraph will be further explored in a separate paper.

2.6 Growing Flat and Convex Surfaces

Before we expand our rule set with the last missing pieces to generate higher genus tilings, let us have a look at some examples for well known abstract polytopes that can be developed already now with the mechanisms of n-colourings, gyres and our simple growth strategy.

We start off by returning to our already known example, the cubical graph, for which we showed the performance of the transpositional colours starting from an already given set of six tiles. This time around, we would like to build it from scratch.

Assuming that we would not know anything about the previous example, we would need to pick the n-colouring, we want to grow the tiling with. Of a cubical graph we know, that it is made up of six quadrilateral faces coming together in eight vertices, three faces per vertex. Based on this information, we can search for an n-colouring that would be able to accommodate the topological features of the cubical graph. Naturally we would narrow the search to the index of 4-colourings in table 7 and check the *Tile-Vertex Incidence* column for entries that points to 4-colourings,

which allow precisely three tiles to come together in all of the vertices. Only one such entry ([3, 3, 3, 3]) can be found in the list, implying that our only hope to grow a cubical graph rests on the combinatorics of $t^{12}f$.

Following our proposed growth strategy from above, we start with a single $t^{12}f$ tile, see figure 9a. The first iteration adds further $t^{12}f$ tiles one by one along the open half-edges, such that no further tiles can be added around the vertices incident to the open half-edges and thus all gyres are realized. This will add four new tiles to our tilegraph.

As before, our tilegraph now again has four open half-edges but this time every edge comes from a different tile, figure 9b. We iterate again and see that only one more tile can be added, since the glueing of the tile to any of the open half-edges leads to an immediate zip-up and leaves the tilegraph with no edges to add further tiles to.

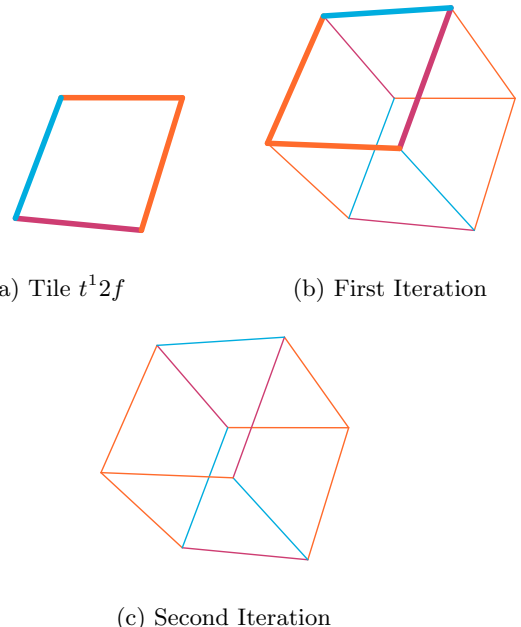


Figure 9: Cube Growth

The undirected version of the resulting tilegraph consists of eight vertices, 12 full-edges and 6 tiles. A cubical graph⁴ (Figure 9c).

We would like to emphasize the somewhat astonishing fact, that the cubical graph appears to be the attractor for the combined system of n-colouring, glueing rules and growth. No other parametrisation than the n-colouring choice was added to the system.

Proceeding using the same mechanism, we can find several other n-colourings with well known spherical tilings as inescapable attractors. t^1 grows a trigonal hosohedron, $3f$ the tetrahedron, $2t^1$ the rhombic

⁴For simplicity's sake we draw our results as an undirected tilegraph. Unglued half-edges will be shown as thick undirected lines while glued half-edges (full-edges) will be shown as one single thin undirected line.

dodecahedron and $2t^1f$ the dodecahedron (see figure 10).

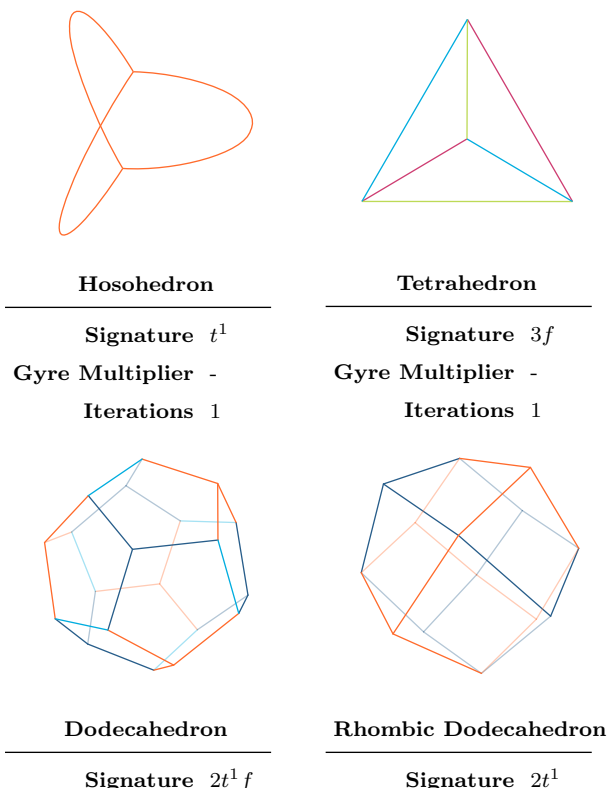


Figure 10: Regular Spherical Tilings

Another interesting example of a finite attractor for the growth of a n-colouring is the triangular bipyramid based on t^1f . It gives us the opportunity to demonstrate the effect of defining a multiplier on gyres. As can be taken from figure 11, the triangular bipyramid sports one monogyre ($gyre_1$ consisting of $t_1(kaki)$) situated at two antipodal vertices and a polygyre ($gyre_2$ consisting of $t_1(kaki)$ and $f_1(cyan)$) at the remaining three vertices.

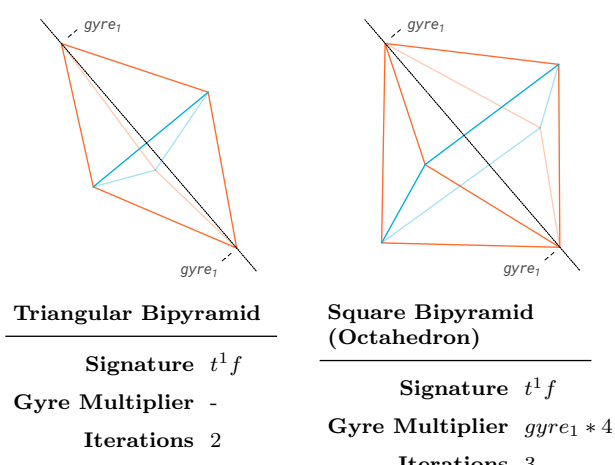


Figure 11: Bipyramids

As has been mentioned before, the possibility to define a multiplier is particularly helpful in the case of monogyres, since their structure allow the degree of the vertices in their pivots to be incremented in steps of one. In the example at hand this enables us to define any degree ≥ 3 specifically for $gyre_1$ and thus to grow t^1f into any bipyramid, including the octahedron (square bipyramid).

Figure 12 shows that a similar method can be applied to create all trapezohedra, since the cubical graph displays the same kind of monogyral bipolarity as the triangular bipyramid. Of particular interest is the pentagonal trapezohedron featured in the figure, because of its relationship with our last missing prominent platonic polytope, the icosahedron.

Topologically, the pentagonal trapezohedron tilegraph is only missing a subdivision of all its regular faces, a chord always connecting the same two vertices in the 4-coloured tile, for its undirected tilegraph to become isomorphic with the icosahedron. Such an internal subdivision of a tile we call an infratiling.

We will discuss this concept and the pentagonal trapezohedron in section 2.8, but first we will turn to finalizing our rule sets and tools to encompass the elements needed for the generation of surfaces of genus > 0 .

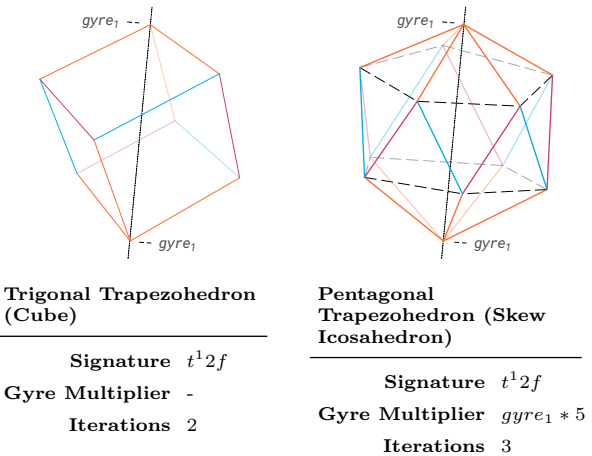


Figure 12: Trapezohedra

2.7 Growing Higher Genus Surfaces

We can imagine two different ways of changing a tilegraph's structure by the glueing of tiles. We can either extend the tilegraph by adding a new tile or we can let it bend in on itself by glueing together tiles already in the tilegraph.

We distinguish between

- **Additive operations** which add a tile to an existing tilegraph
- **Looping operations** which loops a tilegraph by glueing its tiles together along open boundary edges

Both these operations are based on glueing tiles together and are indistinguishable on a local inter-tile level. The effect on the global topology though is fundamentally different. Specifically, looping adds to the genus or has no impact, while tile additions will decrease the genus or leave it in place.

We sketch a proof by showing that an addition of a tile to a tilegraph can only lead to a change of the euler number in the order of $0 \leq \Delta\chi \leq 1$ and the looping of a tilegraph can only lead to $-1 \leq \Delta\chi \leq 0$.

- Any addition of a tile to a tilegraph will as per *simplex rule* initially lead to the addition of $V = n - 2$ vertices, $E = n$ edges and $F = 2$ faces⁵ and thus cannot per se reduce the euler number, the change being $\Delta\chi = V - E + F = 0$.
- Any single step of a zip-up induced operation will result in the reduction of the number of vertices by $\Delta V = -1$, the number of edges will stay the same $\Delta E = 0$ and the number of faces will increase by 2 in the case a hole is closed⁶ and by 1 if not $\Delta F \geq 1$. Thus the change for the euler number will be $0 \leq \Delta\chi \leq 1$ and it follows that the genus will go down by the maximum of 1, since only one hole can be closed per iteration. The only case where a zip-up within several holes can occur due to one initiating operation is when a boundary is glued to itself and thus split into two. A closure of either of these holes would imply though, that a zip-up of the iteration before the looping was not applied, in violation of the glueing rules.
- Consequently, if a zip-up is induced by an addition, the net change of the euler number can be either 0 or 1.
- Looping will initially lead to one new face $\Delta F = 1$ between half-edges, no new edges $\Delta E = 0$ and the reduction of the vertices in the tilegraph by 2 $\Delta V = -2$. Thus the euler number decreases by 1 $\Delta\chi = V - E + F = 1$ and the genus goes up. So when combining the initial increase of genus, caused by a looping operation with a possibly decreasing effect on the genus of subsequent zip-ups, we see that the two can cancel each other out. The net change of the euler number would be 0 or -1 as predicted.

2.7.1 Natural Extension of Rules

While we have already stated that the looping operation locally obeys the already defined glueing rules, we still need to define how these loops are to behave at a distance, their generating rule or in other words how we are to encode the loop growth behaviour.

Just as the colours of the n-colouring encodes the local growth, we continue to use colours as a means to define how loops are to develop. To this end, we

⁵Also counting the face between the half-edges

⁶A hole being a connected set of open half-edges

apply the edge or cross-tile walks already encountered during our definition of the gyre order. See figure 6. We start with some definitions.

Loop Walk A circular walk from edge to edge across multiple tiles in a tilegraph. Due to the *colour rule* and the circularity of the walk, it can be reduced to a cycle of exit edge-colours for every tile on the walk.

Looping Cycle A directed cycle of exit edge-colours taken from the set of colours of a n-colouring. Whereby there is no restriction on how many times a colour can appear. It defines the loop walk.

Looping Unit And Multiplier A looping multiplier indicates the repetition of a looping unit - a sequence of colors, within a looping cycle.

Inverse Looping Cycle The inverse of a looping cycle is the directed cycle of exit edge-colours that inverts the direction of a circular walk. It can be obtained by inverting the sign of any transpositional colour and the sequence of colours in a looping cycle. It defines the inverse loop walk.

Looping Cycle List A sequence of looping cycles assigned to a tilegraph as the combinatorial structure of the looping rule. The sequence defines the order in which looping cycles are to be applied.

Looping Notation We denote the looping cycle list as $L_c = \{loop_1, \dots, loop_n\} = \{(c1_1, c1_2, \dots, c1_q), \dots, (cn_1, cn_2, \dots, cn_x)\}$ with $c1_r$ to cn_x being the colours in the looping cycles $loop_1$ to $loop_n$. To shorten the notation, we can use the looping unit and looping unit multiplier like so $(c1_1, c1_1, c1_1) \equiv 3*(c1_1)$.

Based on the definitions above, we define the following simple looping rules.

Ubiquity Looping Rule This rule declares that any loop walk along the looping cycles must be realized, as soon as the necessary tiles are available in the tilegraph. Looping rules are binding. Specifically after every addition of a tile, following the order of the looping cycle list, we glue the added tile to any other tile in the tilegraph, if this would create a loop walk as defined by a looping sequence, which the newly added tile could be a part of.

Forward Looping Rule No looping cycle is allowed where two consecutive edge-colours in the cycle would lead to an exit of a tile via the edge of entry. Therefore, the same fixed colour cannot succeed itself in the cycle and two subsequent entries of the same transpositional colour must have the same sign.

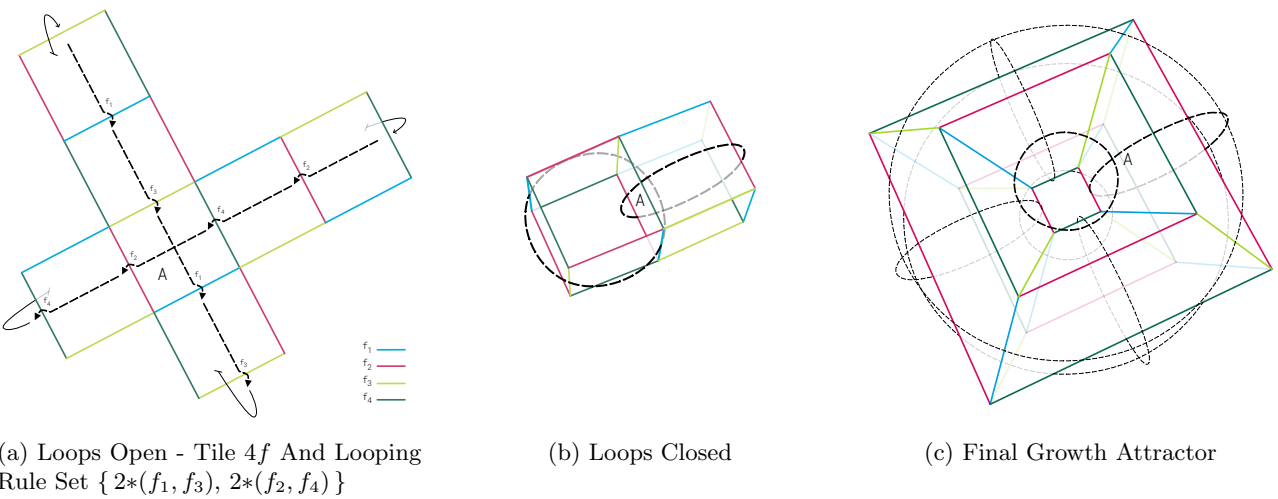


Figure 13: Simple 2-Torus

Figure 13 shows an example of how a simple torus made up of $4f$ tiles is defined by the looping cycles $2*(f_1, f_3)$ and $2*(f_2, f_4)$. Subfigure 13a demonstrates how the edge walks defined by the looping cycles would play out on an unfolded surface, while subfigure 13b reveals how these tiles would be folded based on the rules. Subfigure 13c then reveals the inescapable attractor when applying our rules of growth, glueing and looping to the selected looping cycles and tile colouring.

We observe the following in relation to the just described looping rules.

- Since the *ubiquity looping rule* is binding for all loop cycles in the defined looping cycle list, a situation where the application of a previous looping cycle in the looping cycle list would lead to the impossibility of closing a later looping cycle in the sequence, will be considered a dead end for the growth of the tilegraph.
- All looping cycles and their inverse looping cycles are applied to any single tile in a tilegraph and all tiles will be crossed in any possible way by these cycles. Thus it is important to note, that the crossing of walks seen in tile A of subfigure 13a occurs in every tile of the resulting surface.
- A gyre can be seen as a special case of a loop, which has a vertex rather than edges as one of its two tile sequence boundaries.
- Cross-tile walks incorporating vertices where vertices are addressed using colours of the adjacent edges could also be an interesting future path of inquiry. In such a scenario, the results from the pivot and gyre bound relationships of vertices could be leveraged, but this added complexity is saved for consideration in a later paper.

Before we complete the section on higher genus tilegraphs with some well known examples, let us add some further definitions.

Monoloops Any loop described by a looping cycle containing only one single transpositional colour and no fixed colors is a monoloop.

- If we isolate the tiles along one monoloop in a sub-tilegraph, any tile in the sub-tilegraph will always contribute the same edge-colours to the two different sub-tilegraph boundaries and the two boundary sets of edge-colours will be disjoint.
- The monogyre can be seen as a special case of the monoloop for which one of the boundaries of the sub-tilegraph induced by the monoloop will be a vertex.
- The reverse cycle of a monoloop is equivalent to the monoloop.

Fixed Loops Any loop described by a looping cycle containing only fixed colours is a fixed loop.

- The reverse cycle of a fixed loop is equivalent to the fixed loop.

Mixed Loops Any loop described by a looping cycle containing at least one fixed colour and a transpositional colour or at least two different transpositional colors, is a mixed loop.

- The reverse cycle of a fixed loop is not equivalent to the mixed loop, due to the fact that the same transpositional colour always occurs twice in an n-colouring.

2.7.2 The Toroidal 120-Cell

So far we have only seen examples of finite tilegraphs with relatively low tile count. That the generated surfaces are not limited to these rather simple specimens, can be shown with an example of a finite surface tiled by the pentagonal tile t^1t^2f , which we conjecture to be the wrapping of the 120-cell in such a way that the 120-cell becomes a finite skeletal graph in a one labyrinth sense[8] of the resulting

tilegraph.

120-cell[3].

The t^1t^2f tile itself exhibits local topological properties best expressed by its different gyres. A monogyre of incoming degree 3 and 2 polygyres of degree 4. The higher genus non-local properties of the resulting tilegraph are defined with two loop cycles $3*(t_2)$ and $5*(t_1+, f_1)$.

Figure 14 follows the growth of the tilegraph and its irregular embedding into E^3 step by step using the Kamada-Kawai algorithm[6]. We see how iteration 1 already leads to a first closing of loops, while iteration 2 exposes the tilegraph's first topological branching into 3 separate directions equivalent to the edge branching of the 120-cell at its nodes. Iteration 5 captures the first formation of the wrapped 120-cell's polygonal rings, which can be seen even more clearly in Iteration 6.

The first wrapped dodecahedral cell emerges in iteration 9. Iteration 17 marks the inflection point in terms of the number of tiles added in one step with 1248 tiles being added, after which the steady increase in tension (difference in edge lengths from iteration to iteration), stemming from the impossibility of placing connected vertices equidistantly in E^3 , becomes more and more apparent. Especially iteration 21 testifies to the angle deficit in the nodes of the 120-cell skeleton by showing how the pentagonal rings of the same combinatorial make up display very different dimensions.

Iteration 26, then, marks a second inflection point, where the embedding algorithm pulls the remaining boundaries together inside the approximately spherical extents of the previous iterations and sets the stage for the completely closed tilegraph of 9600 vertices, 18000 full-edges, 7200 tiles and genus 601 after iteration 30.

The supposition, that we are here seeing a wrapping of the 120-cell, is supported by the following arguments.

The tilegraph t^1t^2f with looping cycles $(3*(t_2), 5*(t_1+, f_1))$ consists of 600 subgraphs made up of 12 5-gons with 4 open boundaries defined by the loop $3*(t_2)$. Each of these subgraphs can be seen as the wrapping of a node of the tilegraph's skeletal graph (not to be confused with the tilegraph itself), which allow the skeletal nodes to connect through its 4 open boundaries to adjacent nodes. Thus we get a skeletal graph with 600 nodes of degree 4. These nodes are again organized in cycles of 5 nodes by $5*(t_1+, f_1)$ giving the skeletal graph a girth of 5. As a skeletal graph, we thus have a 4 regular graph with 600 vertices and girth 5, hinting at the relationship with the 120-cell. To complete the picture, we calculate[7] the order of the uncoloured tilegraph's automorphism group to be

$$|Aut(T)| = 120^2 = 14400$$

matching the order of the automorphism group of the

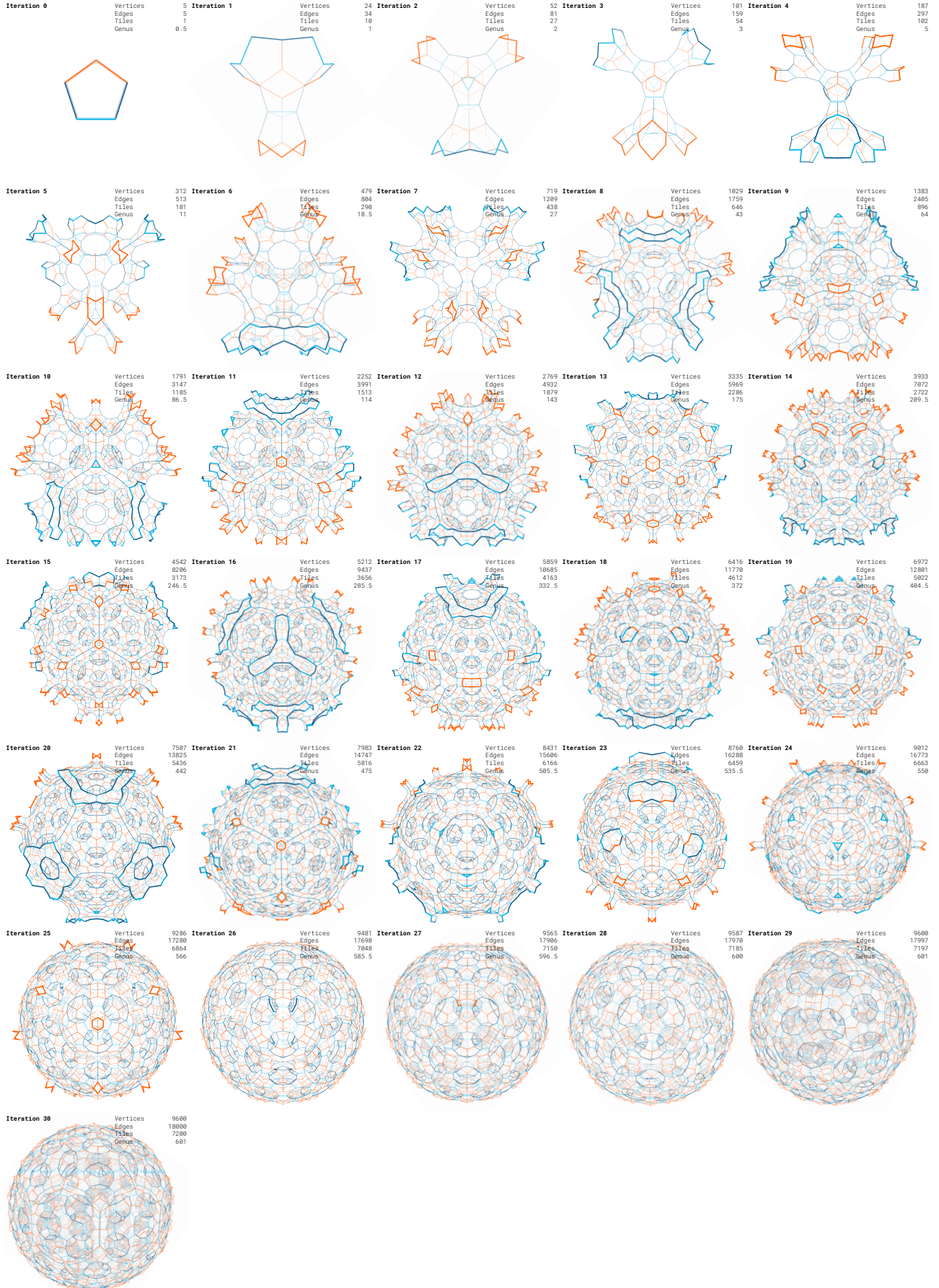


Figure 14: Growing Tile t^1t^2f With Loops $5*(t_1+, f_1)$ and $3*(t_2)$

2.7.3 The Klein Quartic

A further interesting and extensively studied example of a higher genus surface, which can be generated by the system of n-colourings, rules and looping cycles defined above, is the Klein quartic.

We will start our discussion of the Klein quartic by listing some of its well known properties. This will allow us to make informed decisions on what n-colourings and looping cycles to consider when developing the surface bottom up.

We know that the Klein quartic

- is a compact Riemann surface of genus 3 with the highest possible order automorphism group of 336 automorphisms
- admits a regular tiling by 24 heptagons each meeting with 3 others in 56 vertices
- has a tetrahedral skeletal structure

Naturally, we start by looking for tile candidates with gyres of degree 3 in the 7-colourings table 10 under section 4.6 of the appendix to match the known regular tiling. These characteristics are of course the same needed when wanting to grow the 7,3 tiling of the hyperbolic plane. We find that exactly two n-colourings exhibit these particular properties: t^1t^33f and its inverse t^1ft^32f .

From the characteristics listed above, we know that the closed quartic will have a genus of 3, this leaves us with the need to define the loop cycles necessary to self-connect the growing tilegraphs in such a way that they close up and form a genus 3 tilegraph using the 24 allowed tiles. Interestingly, it turns out that there are several tilegraphs fulfilling this requirement, even if we restrict ourselves to only one of the tile 7-colourings found. Thus we will need to calculate the order of the automorphism group as well to authoritatively determine, which of the found topologies are actually the Klein quartic we are looking for.

Table 2 shows three different tilegraphs, the last one being the Klein quartic, strongly twisted in by its embedding. As can be taken from the table, the local symmetries (gyres), the number of vertices, edges and faces as well as the genus do not differ amongst the three. Only the varying looping cycles make the difference in terms of the order of the automorphism group and are responsible for the way the fully grown tilegraphs are twisted in their embeddings. So all the different looping cycle sets are valid choices, when the goal is to generate tilegraphs covering all needed properties for the Klein quartic, but for the automorphism group order. Even more such examples exist.

Since none of the presented tilegraphs have a regular embedding in E^3 , an unfolded version is provided for each one, displaying the 24 tiles in the hyperbolic plane and showing all looping cycle walks

through the central tile A . The cycle walks have been reinterpreted geometrically as curves passing through the midpoints of the coloured edges.

Truly astonishing is the regularity and coverage achieved with just one looping cycle in the case of the Klein quartic. In the depiction of the quartic in the hyperbolic plane, we see that the four different intervals in the looping cycle lead to the four different ways the same curve runs through the central tile A . Together with the fact that this is of course the case for any tile in the tilegraph, this gives an indication of the complexity of the effects a relatively simple looping cycle can already promote.

Furthermore, it can be observed that the curves always run through edges alternately 3 elements down or up the colour cycle, indicating that this specific looping cycle can be thought of as describing a constantly curved geometric path in the embedding of the tilegraph by combinatorial means.

Similar constant curvature paths are also described in the two other examples along the monoloop cycles of colour t_2 and even a straight line can be made out in the fixed loop cycle $3*(f_2, f_3)$, such that one must ask the question, whether the existence of such a thing as combinatorial curvature can be postulated, which directly influences geometric embeddings of tilegraphs. Such a curvature could inform rules of combination and equivalence between looping cycles and possibly be used as a stepping stone for the definition of algebraic structures on the tilegraphs.

What is safe to say though, is that further indicators of specific topological properties, like for example the gyre degree, would be extremely helpful in the targeting of specific desired outcomes within the vast space of possible solutions. Especially since, when one examines the number of tiles crossed with the loop cycles of our three examples at hand, one cannot help but wonder how the inner tetrahedral structure comes about for the Klein quartic by only defining four tile cycles. The looping cycle for the quartic cannot be said to be an obvious experimental choice, at least when approaching the problem with the tools we currently have.

For the central example in table 2 the chosen looping cycles appear to be much more natural. Predicting the growth of the tilegraph seems much more intuitive, seeing that we have almost perpendicular looping cycles, we can attribute the tighter loop with wrapping the edges of the skeletal tetrahedron and the wider loop tracing the edges around the skeletal faces, expending 2 of its 6 tiles per node along the way.

Also the leftmost example lends itself to a similar analysis, albeit with a more skew wrapping of the skeletal edges by the t_2 monoloop, which needs to be accounted for by the mixed loop. The famously twisted Klein quartic seems much less approachable. To sharpen our intuitions, we therefore want to expand a bit on how the looping cycles become capable of winding up tilegraphs.

n-colouring	t^1t^33f	t^1t^33f	t^1t^33f
loop cycles	$3*(t_2), 2*(t_2+, f_2, t_1-)$	$2*(t_2), 3*(f_2, f_3)$	(t_1-, t_2+, f_3, f_1)
vertices	56	56	56
edges	84	84	84
faces	24	24	24
genus	3	3	3
auto group order	24	24	336
	Tetrahedral	Tetrahedral	Klein quartic

Table 2: Multiple Genus 3 Tilegraphs with 24-Tiles

2.7.4 Winding

The biggest hurdle for understanding combinatorial winding intuitively is that it most explicitly manifests itself in larger tilegraphs. These structures are hard to grasp even when regularly embeddable in E^3 . And even in simpler tilegraphs like the one exhibited in figure 13c, effects of the looping cycles are far from easy to interpret. Nevertheless, the 2-Torus is a good starting point for exploring what the possibilities and naturally given boundaries are for the definition of winding via looping cycles.

Figure 13c shows such a torus based on $4f$ and defined by the looping cycles $2*(f_1, f_3)$ and $2*(f_2, f_4)$. Imagine cutting it open along one of the connected edge cycles of *cyan*(f_1) and *lime*(f_3) edges. We thereby receive two open boundaries containing two *lime* edges and two *cyan* edges each. It is easy to see how this boundary could be re-glued in two different ways, recreating the previous version of the tilegraph or a new more twisted version by flipping the *cyan* and *lime* edges being connected.

Phenomenologically, one could describe the second version of the 2-torus as what you get, when you

twist the open boundaries by a half turn against each other and then glue. The extrinsic topology does not change, since we still have a 2-torus in both cases, but the intrinsic structure does, analogically to the tilegraphs in our Klein quartic table.

Seeing that a second kind of glueing is possible, we can now look for the looping cycle needed to replace $2*(f_1, f_3)$ ($2*(cyan, lime)$) in order to describe a walk connecting the *cyan* edge with the alternative *cyan* edge along the matching edge boundary. Such a walk is shown in figure 15a.

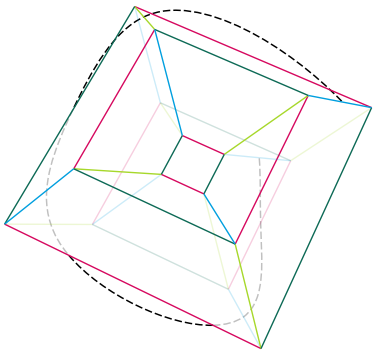
The question of course arises whether we can stay with this geometric interpretation of the re-glueing and go even further imagining rotating the two boundaries with a full turn against each other. The boundaries would be reconnected in exactly the same way they were before the cutting, with the difference that the whole torus would perform a full twist. Does a looping cycle exist, that would be able to define this kind of twist?

The answer is yes and no. A looping cycle describing a full turn is possible and even fairly easy to come up with $2*(f_1, f_2)$ ($2*(cyan, wine)$), but the result is not what we might expect, a 2-torus twisted once.

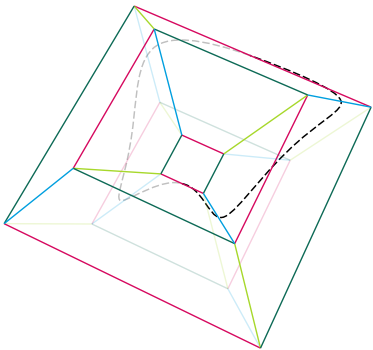
Rather we get a 2-torus isomorphic to our initial torus with a looping rule describing a curve that winds one more time about the torus instead.

As soon as we connect the same edges and vertices again, there is no combinatorial or topological difference to our initial torus (see figure 15b). Whether this observation also holds for more complex scenarios beyond the torus, which also take the growth of the tilegraphs into account, is still an open area of research.

Evidently, with a growing number of colours in the base n-colouring the possibilities for defining looping cycles with different windings increase.



(a) Half Turn Alternative



(b) Full Turn Isomorphic

Figure 15: Alternate Winding

To further illustrate the intricacies of windings on tilegraphs, figure 16 shows some sample walks along different colour sequences on a bone-like embedded tilegraph. The tilegraph is based on the same tile t^1t^33f we already used in our Klein quartic exposition.

Were we to close the displayed walks/sequences to loop cycles after one or more iterations, and use the resulting colour cycles as input to looping rules, the tilegraphs grown from this input would seemingly differ substantially, judging from the different courses they take. Predicting which of these sequences would lead to differing results however, turns out to be no easy feat.

Examining the figures closely, we for example see that the figure 16d and figure 16f display sequences starting and ending at exactly the same $f_1(\text{cyan})$ edge

within the same bone opening.

One might jump to the quick conclusion, that using them as looping cycles, would achieve the same glueing between multiple bone like structures and thus the resulting tilegraphs would grow and develop in the same way. This in accordance with the observed behaviour in the torus example above, where more than a half twist could not be achieved by increasing the winding of the looping cycle around the tilegraph.

If we inspect the course of the two drawn sequences colour for colour, though, we see that the sequence in figure 16d always crosses $f_1(\text{cyan})$ with the same preceding color, while the sequence in figure 16f crosses $f_1(\text{cyan})$ after two differing colors. Consequently, the sequences will branch differently at $f_1(\text{cyan})$ and tilegraphs resulting from using the sequences as looping cycles will differ also.

Without going into more depth and developing the examples in figure 16 further, we can make three general observations.

First off, it becomes apparent how the combinatorial structure of the tilegraph's coloured edges can be used as a means to describe combinatorial curves on the surface, be they closed cycles or open and infinite. Needless to say, that these curves can be ported to the metric spaces of the tilegraph's embeddings and studied further there.

Second, colour sequences can describe windings around tilegraphs, whether the sequences have been used as generative input for the tilegraphs underlying looping rules or are simply studied as an expression of the tilegraphs combinatorial structure.

And last but not least, figure 16 again amply illustrates how different looping rule colour sequences, result in different large scale structures.

2.8 Infratilings

Until now we have been content with treating our tiles as graph cycles with no inner edge structure. Not discussing for example the possibility to add chords to our n-coloured tiles, except for a short interjection regarding the relationship between the pentagonal trapezohedron and the icosahedron. Adding further structure though adds potential in several areas.

Since any graph cycles of $n \geq 4$ per definition allow for straight edge embeddings of tilegraphs consisting of skew polygons, subdividing the tiles used, for example by triangulation, would allow us to transform a skew tilegraph embedding into an embedding of a tilegraph discretely bounded by planes.

Furthermore, as was hinted at in the earlier remark, there is also a potential to generate known tilings like the icosahedron by further refining the edge structure of tilegraphs through subdivisions of their base tile.

Very importantly, by adding additional structure to the cycle graphs in the tilegraph, we do not aim to compromise combinatorial regularity on the structural level of the tiles, but rather to add the possibility for lower level combinatorial extensions within the

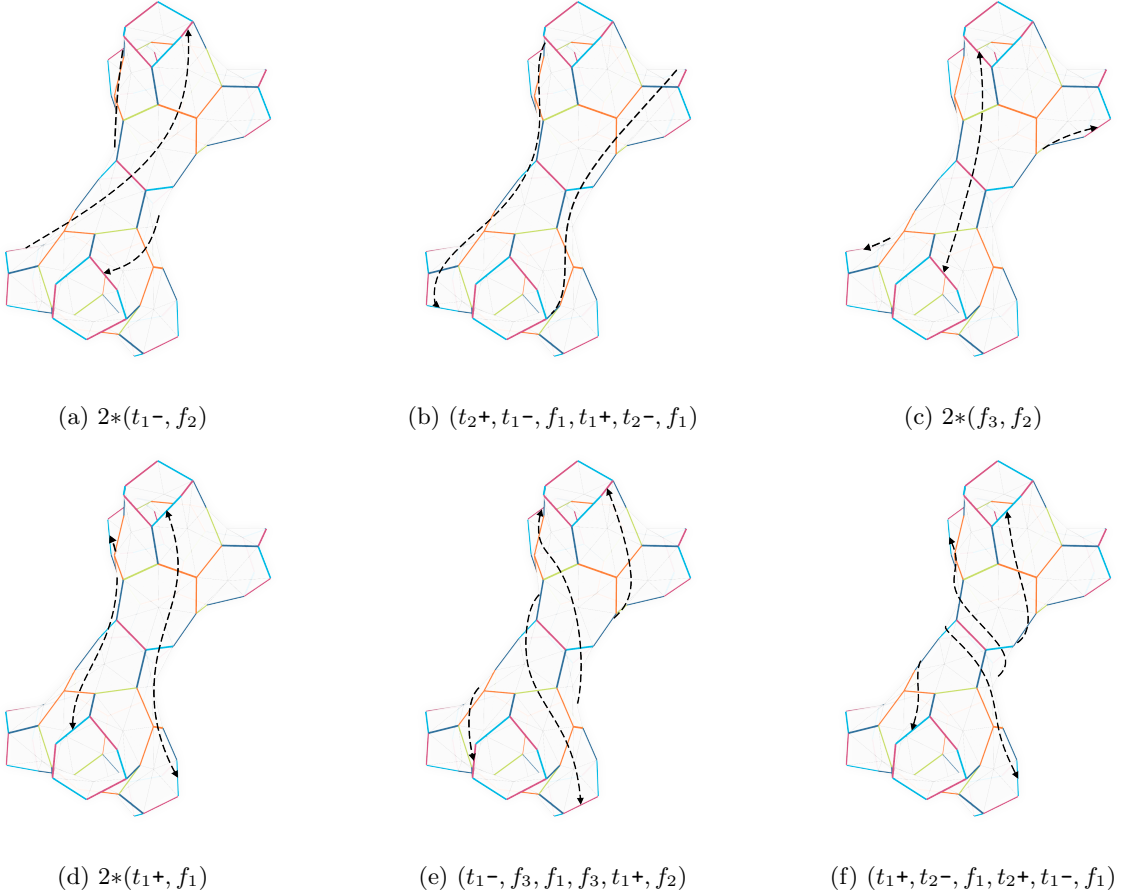


Figure 16: Winding of Different Looping Cycles

tiles.

These extensions can take the same form throughout the tiles in a tilegraph, as well as vary from tile to tile, with which we gain the capability to encode different states of tiles by means of adding combinatorial substructures.

We will refer to such substructures as infratilings. Infratilings can be further described in the following way:

Infratiling Structurally, an infratiling of a tile is a full-edge multigraph with $2 \leq v_l \leq n$ leaf vertices. The leaf vertices must map bijectively to the tile cycle vertices in such a way that the combined graphs result in a connected planar graph within which the tile cycle is still facial. Or geometrically speaking, an infratiling subdivides a tile, embedded as a disc, into several discs.

Centroidal Infratiling A centroidal infratiling is realized with a full-edge star graph connected to at least 3 vertices of the tile cycle graph and zero to several chords.

Chordal Infratiling An infratiling realized only with full-edge cycle graph chords and no added vertices.

Regularly Infratiled Tilegraph A tilegraph containing tiles that all show a substructure

consisting of the same multigraph with the same bijective mapping.

We will explore the benefits the infratilings create in our framework by revisiting the pentagonal trapezohedron and adding the example of the (at least to us) surprising tiling of the two reciprocal compact regular skew apeirohedra $\{6, 4|4\}$ (muoctahedron) and $\{4, 6|4\}$ (mucube) with the same skew 8-coloured tile.

2.8.1 Converting the Pentagonal Trapezohedron to an Icosahedron

As we saw in section 2.6, the base tile $t^{12}f$ generates the pentagonal trapezohedron. In order to define our mapping of the infratiling to the base tile, we will use the vertex labels relative to the tiles. To recap what we wrote under section 2.1.1, the four vertices of the base tile in our concrete example will be named $V = \{v_1, v_2, v_3, v_4\}$ starting with the source vertex of the edge coloured by t_1- , since this is the reference element of the n-colouring. Now that we have our vertex labels in place, we add a simple chordal infratiling by connecting v_3 to v_1 by a full-edge (directed half-edge cycle). The infratiling thus consists of a full-edge edge dividing our base tile into two faces. The same infratiling is applied to all tiles in the tilegraph, always using the vertex labels relative to the tiles.

The unfolded undirected tilegraph in figure 17 illus-

trates how the regular subdivision of $t^1 2f$ leads to an icosahedral net originating in the pentagonal trapezohedron of figure 12.

As can easily be seen, applying the zip rule to the unfolded net will result in two instances of antipodal t_1 monogyres of indegree 5, while the instances of degree 3 mixed gyres will be supplemented with two infratiling edges each and thus also end up as indegree 5. Consequently, we have the desired result of an undirected tilegraph isomorphic to the icosahedral graph, since the ten tetragonal faces of the pentagonal trapezohedron are split into 20 triangular faces with 5 around each of the 12 vertices.

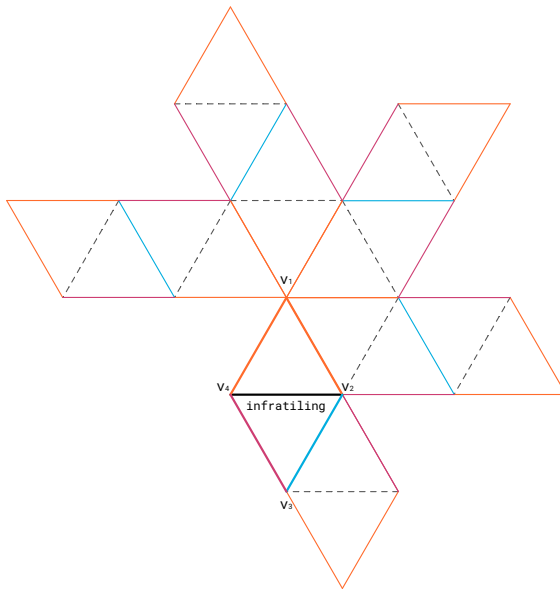


Figure 17: Unfolded Icosahedron with Infratiling

2.8.2 Regular Octagonal Tiling of the Mucube and Muoctahedron

The mutetrahedron - linking six hexagons around each vertex, the mucube - arranging six squares around vertices, the muoctahedron - combining four hexagons around each vertex. All are classic examples of infinite polytopes.

Because of their regularity and due to the extensive coverage their geometrical and combinatorial properties have enjoyed since their discovery[2], they are obvious choices when looking for examples of apeirohedra to describe using our framework.

Finding solutions for the mutetrahedron (tile $6f$ and looping cycles (f_1, f_3, f_5) and (f_2, f_4, f_6)) and for the muoctahedron proved to be quite an easy endeavour (tile $t^2 ft^2 f$ and looping cycles $4 * (t_1), 4 * (t_2), 2 * (f_1, t_2 +)$ and $2 * (f_2, t_1 +)$).

The mucube, somewhat astonishingly, turned out to be much more evasive.

Within our framework we are not bound to think in commonly utilized planar geometric entities like for example triangles or squares as the basic building blocks of our structures, when searching for ways to describe well known polytopes and apeirohedra.

Much rather we can look for meta structures, which can then be further refined using infratilings, as seen in the example of the icosahedron. The search for the mucube proved to be a perfect example of the use of such a procedure.

While representations of the mucube clearly suggest that it is geometrically built upon squares, it was not until we started experimenting with transpositional tiles of more than four edges that a solution was found.

Several approaches were taken based on studies of the mucube geometry, like using units based on skew hexagonal tiles with edges incident to the diagonals of the squares or mapping edges of a dodecagonal tile to the regular edges of the mucube, while letting it cover six squares at a time. Both approaches lead to dead ends. The in our eyes much more unlikely candidate, which we succeeded solving the mapping problem with, was an octagonal tile.

Not only the fact that the transpositional tiling of the mucube should be based on an octagonal meta structure came as a surprise to us, but also the way this tiling helps elucidate the tight geometric and combinatorial relationship between the mucube and the muoctahedron.

The geometry of the skew octagons one would need to be looking for is quite clear.

Take a regular unit square. On two opposing edges of the square add isosceles triangles pointing upwards, away from the square's plane in a 90 degree angle with equal leg lengths of $\frac{\sqrt{2}}{2}$. On the other two edges add the same size triangles pointing down. We thus get a skew octagon by adding four new vertices to the four given by the square.

Four of the triangles added can be combined in a plane to create another square equal in size to our base square. Using this property, we can create a geometric tiling of the mucube, where half the vertices of the octagons would be incident to centres of the mucube squares, while the other half would come to lie on the corners of the squares.

Combinatorially, this means that half the vertices of this new tiling would be incident to four octagons, while three octagons would always come together at the other half of the vertices. As a consequence, the combinatorial requirements of the n-colouring needed were given.

The 8-colouring $4t^1$ shows promise by matching these requirements. This can easily be checked in the 8-colouring table under table 11 or by drawing its gyre graph. Additionally, one could argue that, with four consecutive edge pairs of same transpositional colour, this highly symmetric n-colouring already hints at a tetragonal structure.

In the left hand column of figure 18a, $4t^1$ can be found illustrated as a mapping onto the skew geometry of the octagonal tile described above without any infratiling, while the middle column shows

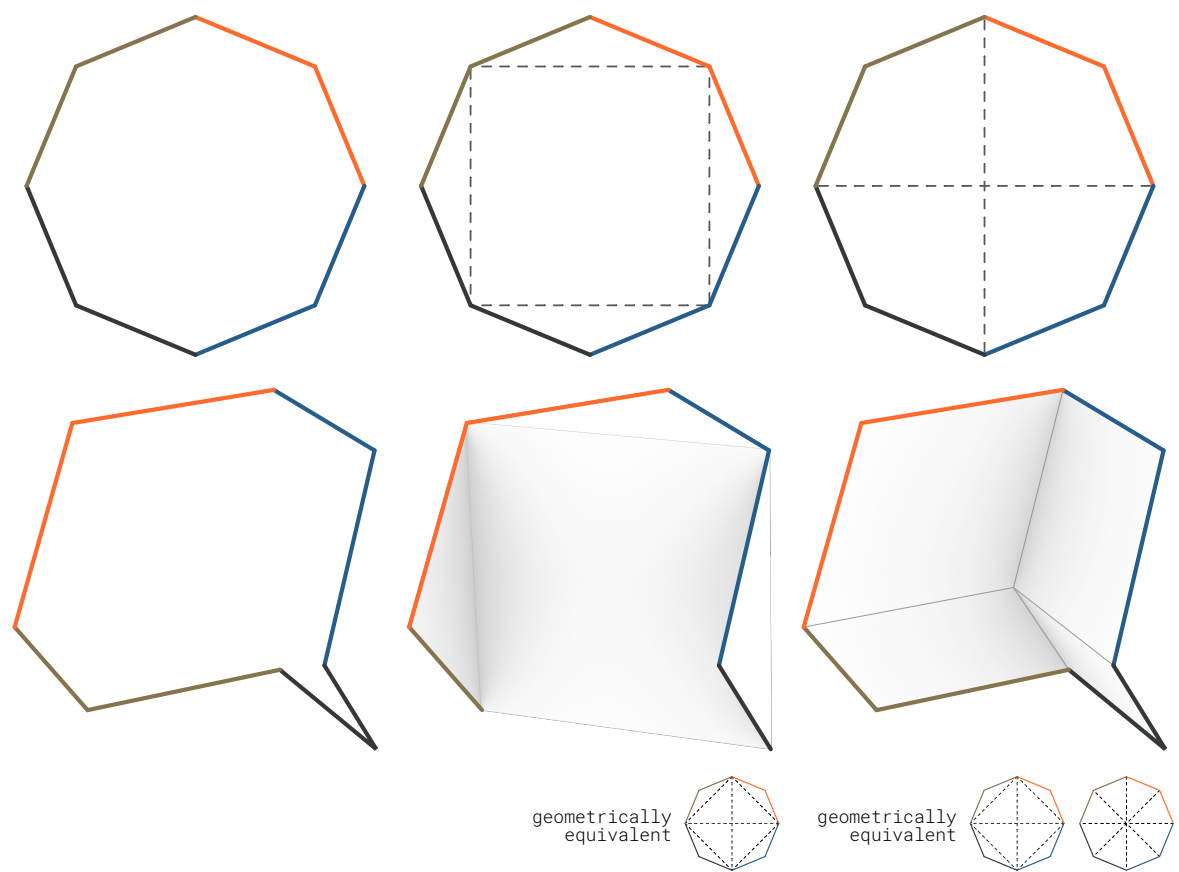
the embedding of the tile, including its infratiling as related to the combinatorial structure. The chosen mapping of the chordal infratiling is essential to guarantee, that the right geometrical properties converge with the combinatorial effects given by the n-colouring and thereby make the covering of the mucube possible.

Armed with the basic combinatorial properties of our tile, we can now search for possible looping cycles and find that $2 * (t_1-, t_4-), 2 * (t_1+, t_2+), 2 * (t_3-, t_2-)$ and $2 * (t_3+, t_4+)$ will create the tilegraph represented in the left most illustration of figure 18c. Combined with the infratiling and geometry of the base tile described above, this tilegraph yields the mucube surface displayed at the center of the figure. Thus our initial goal of creating the mucube using transpositional tiling has been reached.

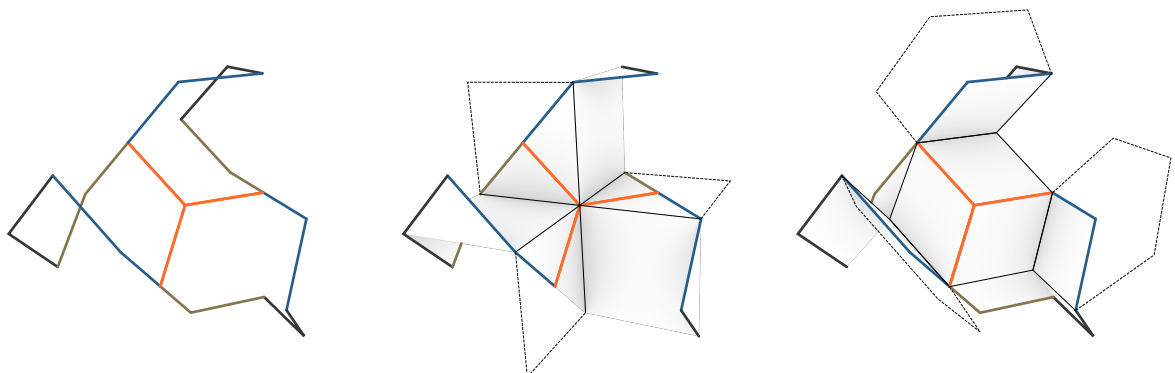
Surprisingly though, not only the mucube is hiding in this octagonal structure, as can be seen in the right column of figure 18, the muoctahedron is also present in the exact same geometric framework spanned by the skew octagons described above.

Quite surprisingly, the only difference between the mucube and the muoctahedron in terms of transpositional topology lies in the choice of the infratiling. We merely need to switch its mapping from the currently targeted four vertices to the alternate four vertices of the octagonal tile and flip the four infratiling edges from a chordal to a centroidal orientation in order to transform the mucube into a muoctahedron. The geometry of the octagon edges remains the same, as can be seen in the center and right column of figure 18a and figure 18b.

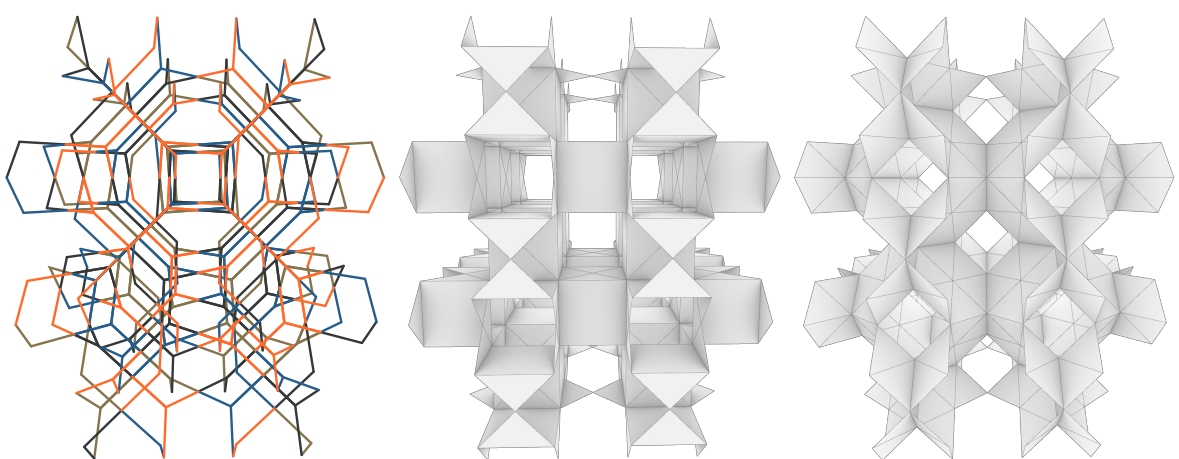
The geometric secret to the example above, was of course already present in Coxeter's notion of reciprocity between $\{6, 4|4\}$ and $\{4, 6|4\}$. The centres of the faces of one become the vertices of the other. We believe though, the ability to describe these two apeirohedra, which seem so intuitively related to squares and hexagons, via the same octagonal scaffolding, to be a beautiful demonstration of the capacity and potential of using transpositional topology to find deeper combinatorial relationships, even in already well known poly- and apeirotopes.



(a) None, Square and Star Infratilings of Tile $4t^1$



(b) Same 3 Tile Arrangement With Different Infratilings



(c) Tilegraph And Resulting Mucube And Muoctahedron

Figure 18: One 8-Colouring Tile With Different Infratilings Resulting In Square Based Mucube and Hexagon Based Muoctahedron

3 Conclusion

With the notion of infratilings, the last fragment of our approach has fallen into place. We have shown how a simple set of glueing, looping and growth rules applied to tiles coloured by two types of colours, intuitively yield tilegraphs mappable to surface tilings as diverse as the dodecahedron, the heptagonal tiling of the hyperbolic plane or the mucube.

Many further examples have already been explored, but presenting them here would have defied the purpose of this exposé, which was to give an introductory overview of our framework and to convey its merits. Admittedly mathematical rigorousness might have suffered from our growing desire to watch these enticing creations grow out of simple coloured cycles. However the complexity and dare we say beauty of the generated structures attest to the resilience of the framework towards theoretical roughness, which is waiting to be ironed out in further publications.

In the end, it was the seductiveness of the tile compositions, hinting at ever more complex structures,

that led us to at the same time generalize and refine the rules and methods used during countless hours of glueing paper tiles or navigating the virtual results in **grasp**, and finally to come up with what we see as an astonishingly approachable system to generate simple as well as complex surfaces.

We believe our basic building blocks - transpositional and fixed colours, n-colourings, gyres and in a certain sense tilegraphs - to be quite well understood within our own system. How they connect to other mathematical systems used to describe symmetry or structure like groups and orbifolds is still very much an open question. Further subjects only superficially broached, like different rules for growth, the interaction of looping, windings and infratilings, also leave a lot of room for further investigation. We hope to fill in some of these areas in future papers but also to have sparked enough interest in our approach for others to participate in refining the framework and its mathematical underpinnings.

We end our elaborations with a set of further examples in figure 19.

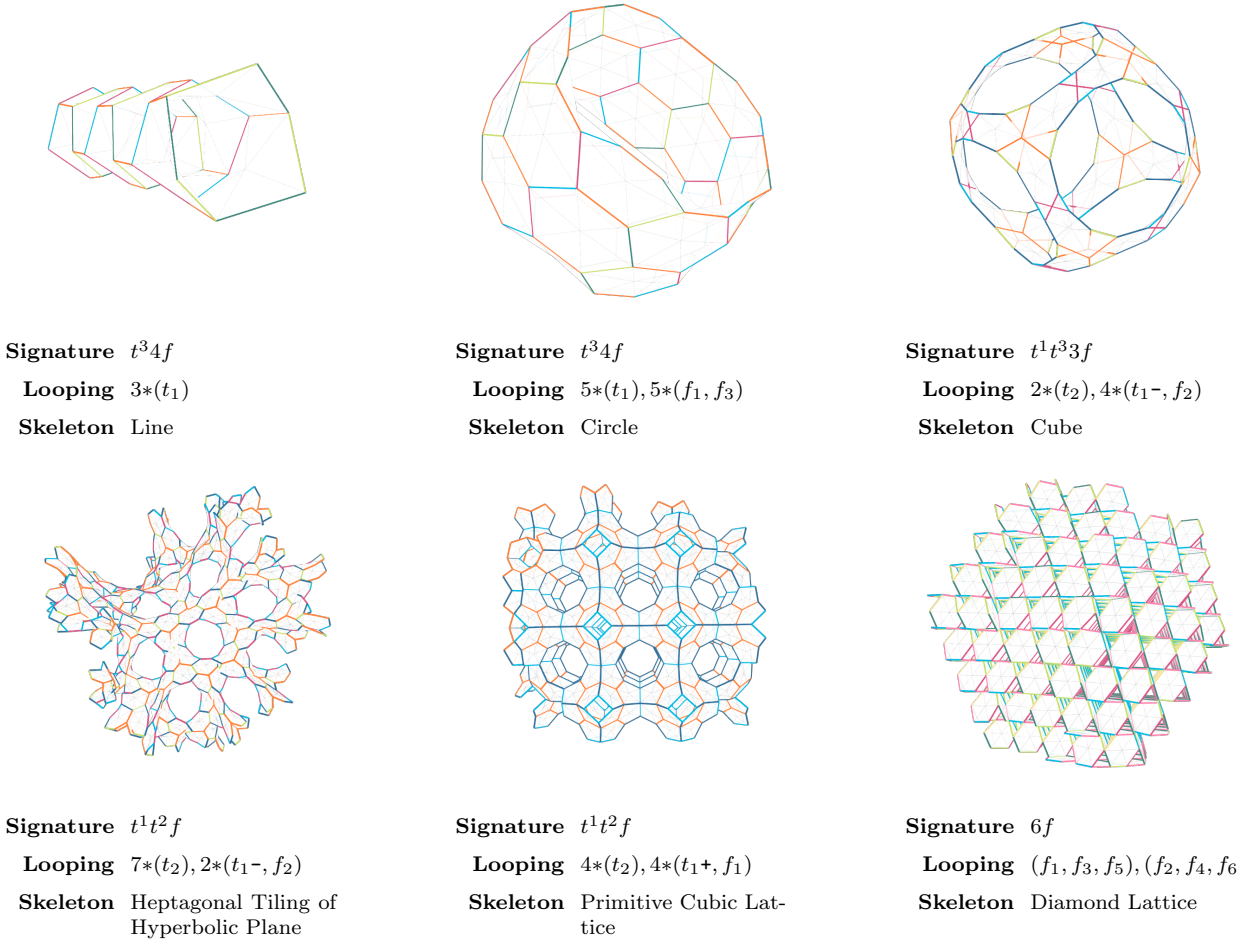


Figure 19: Skeleton Wrapping Samples

4 Appendix

4.1 Definitions

4.1.1 N-Colourings. Their Structure, Index and Signature

Definition 4.1 (N-Colouring).

Let a fixed colour set F_i be a set of i fixed colours $\{f_1, f_2, \dots, f_i\}$

Let a transposition colour set T_j be a multiset of transposition colours t_j with multiplicity 2 $\{t_1, t_1, t_2, t_2, \dots, t_j, t_j\}$

Let a colouring multiset $C = T_j \cup F_i$ of cardinality $n = |C|$ be a union of transposition colour multiset T_j and a fixed colour set F_i where n and j are chosen such that $n, j, i \in \mathbb{N}$ and $0 \leq j \leq n/2$ and consequently $i = n - 2j$

Then we define a specific n -colouring $nCol = [c_1, c_2, c_3, \dots, c_n]$ as a cycle of colours based on the elements of a permutation $P \in S(C)$.

Definition 4.2 (N-Colouring Structure). We define the structure $Struct_{nCol} = [I_1, I_2, I_3, \dots, I_n]$ of an n -colouring as the cycle containing the size of the intervals between any occurrence of an element in the cycle of an n -colouring with its second occurrence. The size of the interval $|I_f|$ of any fixed colour element f will always be the cardinality of the n -colouring n , while the size of the interval $|I_t|$ of any transposition colour element will always be $I_t < n$ and the sum of the intervals of two consecutive elements of the same transposition colour will obviously be n .

Example

The structure of the 5-colouring $c_5 = [t_1, t_1, t_2, t_2, f_1]$ would be $Struct_{c_5} = [1, 4, 1, 4, 5]$

Definition 4.3 (N-Colouring Equivalence). We define two n -Colourings $nCol_{1n}$ and $nCol_{2n}$ as equivalent, if their structures $Struct_{nCol_{1n}}$ and $Struct_{nCol_{2n}}$ are equivalent $Struct_{c_1n} \equiv Struct_{c_2n} \Rightarrow c_1n \equiv c_2n$. So that $[t_1, t_1, t_2, t_2, f_1] \equiv [t_3, t_3, f_2, t_4, t_4]$

Definition 4.4 (N-Colouring Index). In order to define a unique index referencing a specific n -colouring, we use definition 4.3 and define a rule for a cut of the cycle of the n -colouring structure that will always result in a unique linearly ordered set, which can be used to create a unique index.

Let d be the number of digits of n .

Let $Struct_{nCol}$ be a n -colouring structure and thus a cycle. Then $Struct_{nCol}$ can be cut in n ways to create n different linearly ordered sets.

Let $K = \{L_1, L_2, \dots, L_n\}$ be the set of n possible linearly ordered sets created by cutting $Struct_{nCol}$. Then the index is defined by the function $f : K \rightarrow index$ that finds a natural number: $index \in \mathbb{N}$ based on the linearly ordered sets in K with $f(K) = \min(\{\sum_{i=1}^n \sum_{j=1}^n I_j * 10^{d(n-j)} | I_j \in L_i\})$.

Welcome side effects of breaking down the n -colouring cycle into a uniquely defined linearly ordered set are that we can now define conventions for addressing colours in a n -colouring:

- Fixed and transpositional colours are numbered separately starting with t_1 and f_1 for the first element of the respective type in the linearly ordered set, t_2 and f_2 for the next and so forth.
- Additionally, the first occurrence of a specific transposition colour will be marked with a $-$, while its second occurrence will be marked with a $+$.

Definition 4.5 (N-Colouring Index). As an alternative to the somewhat unwieldy index of definition 4.4, we define a more dense and readable signature of n -colourings in the following way.

Starting from the linearly ordered set L_{index} used as a base for the index.

1. Replace all elements of value n (all fixed colour intervals) with an f
2. Remove all second occurrences of transposition colours
3. Replace all first occurrences of transposition colours with a $t^{interval}$ where interval is the value of the element replaced
4. Replace all consecutive equal elements with their consecutive count followed by the repeated element
5. Concatenate all elements in sequence

Example

The linear order of the structure for the 5-colouring $c_5 = [t_1, t_1, t_2, t_2, f_1]$ used as a basis for the index would be $L_{index} = \{1, 4, 1, 4, 5\}$. The resulting signature would be $2t^1f$.

See also the section 4.6.

n-Colouring	Index	Signature
t_1, t_1	11	t^1
t_1, f_1, t_1, f_2	2424	t^22f
t_1, f_1, t_1, f_2, f_3	25355	t^23f
$t_1, t_2, t_1, f_1, t_3, t_2, f_2, t_3$	24683485	$t^2t^4ft^3f$

Table 3: Index and Signature Examples

4.1.2 Algorithm for Enumeration of n-Colourings

The algorithm for finding the entries in the n -colouring index (see section 4.6) is defined in the following way.

Definition 4.6.

Generate one colouring multiset with 0 to $\lfloor n/2 \rfloor$ transpositional colours, labeling the transpositional colours with t_1 to $t_{\lfloor n/2 \rfloor}$ and the $n - \lfloor n/2 \rfloor$ fixed colours with f . A sample set for a 5-colouring would be $\{f, t_1, t_1, t_2, t_2\}$.

For every colouring multiset, generate all possible permutations following the process described in "Loopless Generation of Multiset Permutations using a Constant Number of Variables by Prefix Shifts" [11] by means of the software library multipermute [4]. This leads to an excess of permutations, since this will not take the cyclic nature of the n -colourings into consideration ($\{f, t_1, t_1, t_2, t_2\} \equiv \{t_1, t_1, t_2, t_2, f\}$) and we are not interested in differentiating the transpositional colours so $\{f, t_2, t_2, t_1, t_1\}$ needs to be equivalent to $\{f, t_1, t_1, t_2, t_2\}$. These excess permutations need to be filtered out.⁷

Cycles are filtered by ensuring that a permutation sequence X is not a subsequence of the concatenation $Y + Y$ of another sequence Y .

Permutations stemming from transpositional colour differentiation are removed by comparing the resulting indexes of the permutations.

4.2 Tiles

Definition 4.7 (Tile).

To form a tile, we create a directed cycle graph or directed n -gon similar to its undirected geometrical counterpart the polygon, consisting of n vertices and n directed edges and bijectively as well as sequentially map the elements of the n -colouring to the edges of the graph.

As was seen above, we can break down the n -colouring mapped to the tile to a linearly ordered set. We use this as a basis for numbering the vertices of our tile in the following way. v_1 we define as the vertex at the source of the edge coloured with the first colour in the linearly ordered set, v_2 denotes the vertex at the source of the edge coloured with the second colour in the set and so forth.

4.3 Tilegraphs

Definition 4.8 (Tilegraph).

We define a tilegraph based on base tile B as a directed Multigraph $T = (V, E)$ that consists of one or a combination of multiple subgraphs/tiles isomorphic to B . Two vertices may be connected by up to 2 directed edges with differing source and target vertices.

If in T a directed half-edge (v, u) exists and no inverse half-edge (u, v) we define this edge as unglued. Unglued edges constitute the edge boundary of the tilegraph.

⁷Needless to say that a more efficient direct generation algorithm would be preferable, but we have found none so far, even though at least part of the problem seems well defined within the area of combinatorial necklaces

If in T a directed half-edge (v, u) and a directed half-edge (u, v) exists, we define these edges as glued.

Vertices of T are unlabeled in the sense that they only exist as entities between two colours, thus when we speak of two isomorphic tilegraphs, we only consider the edges labeled by the colouring of the tiles and the structure of the graphs.

4.4 Gyres

Definition 4.9 (Gyre).

Let the complete edge-neighbourhood $N_{eT}[u]$ in a tilegraph T be the subgraph induced by the edges incident to vertex u in tilegraph T . We call $N_{eT}[u]$ complete if the edge-neighbourhood consists of full-edge cycles (half-edges pairing up to full-edges).

As per the colour rule, any full-edge cycle in a Tilegraph must consist of two edges of the same fixed colour or of two edges of the same transpositional colour with opposite signs $+, -$ and per the self-connect rule the half-edges cannot be part of the same tile.

As per the glueing rules, any tile A_i with edges in $N_{eT}[u]$ will contribute one and only one pair of adjacent edges $e_n, e_{n+1} \in E(A_i)$.

We define the gyre of the vertex u in Tilegraph $T = (V, E)$ as a cycle R of edge-colours $c(E)$ of the complete edge-neighbourhood $N_{eT}[u]$. The order is defined in the following way:

1. We pick any inbound half-edge $(n_1, u) \in N_{eT}[u] \cap E(A_1)$ and add its colour $c((n_1, u))$ to the gyre R as the first element.
2. The second colour in R will then be the following outbound half-edge $(u, n_2) \in N_{eT}[u] \cap E(A_1)$.
3. The third colour will be the colour of the inbound half-edge of $(n_2, u) \in N_{eT}[u] \cap E(A_2)$, the fourth the colour of the outbound half-edge of $(u, n_3) \in N_{eT}[u] \cap E(A_2)$.
4. We continue adding colours to R following the procedure as described in 1-3 until the number of inbound edges is at least 3 for regular pivots in order to uphold the zip-up rule or at least the pivot degree $u_{td} \geq 3$ and we reach the paired half-edge of (n_1, u) which is $(u, n_1) \in N_{eT}[u] \cap E(A_x)$.

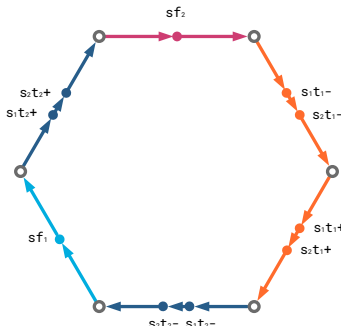
Definition 4.10 (Gyre Graph Construction). Let a gyre graph denote the expansion of a n -coloured cycle graph of a tile G with $E(G) = \{e_1, e_2, \dots, e_n\}$ and $V(G) = \{s_1, s_2, \dots, s_n\}$ in the following way:

1. We splice a gyre vertex s_{f_i} into any edge coloured with a fixed colour, while maintaining the cycle of the digraph. Such a vertex will be referred to as a fixed vertex.
2. We splice two gyre vertices $s_{1t_i+/-}$ and $s_{2t_i+/-}$ into any edge coloured with a transpositional

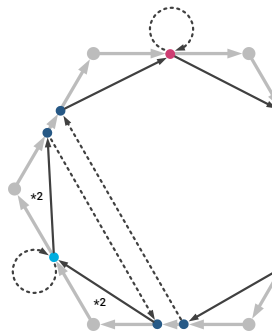
colour, while maintaining the cycle of the digraph. Such gyre vertices will be referred to as transpositional vertices and will be ordered in the direction of the digraph.

3. Starting from every fixed vertex sf_i and every transpositional vertex $s_2t_i+/-$, we add a directed chord to the next gyre vertex following along the cycle of the n -colouring.
4. For every fixed vertex sf_i we add a directed loop (sf_i, sf_i) .
5. We add two directed chords to the cycle for every transpositional colour, connecting s_1t_i+ of the "+"-edge with s_2t_i- of its corresponding "-"-edge and s_1t_i- of the "-"-edge with s_2t_i+ of its corresponding "+"-edge.

Additionally, by removing all coloured edges and keeping only the directed chords, the different gyres can be isolated as components of the gyre graph. See figure 7 as an example



(a) Splicing



(b) Added Chords

Figure 20: Gyre Graph Construction

4.5 Growth Examples

In this section, we show various examples of using different growth mechanisms. We will limit ourselves to a small set of examples to illustrate the defining impact the choice of the initial seed of tiles and the iteration process has on the resulting tilegraph.

4.5.1 Tile Doubling by Induced Zip-Up

This example shows how even in a purely additive context dead ends can occur due to the zip-up rule. We set the stage for our demonstration as follows. Let $S = \{A_1, A_2, \dots, A_{12}\}$ be a set of twelve tiles of n -colouring $t^2t^3t^2$.

1. We glue A_2 via its t_1- (*kaki-*) edge to A_1 's t_1+ (*kaki+*) edge and A_3 via its t_1- (*kaki-*) edge to A_2 's t_1+ (*kaki+*) edge to get a sequence of three tiles.
2. To A_3 t_2- (*navy-*) we glue A_4 and to A_4 t_2- (*navy-*) we glue A_5 .
3. To A_5 t_1- (*kaki-*) we glue A_6 and to A_6 t_1- (*kaki-*) we glue A_7 .
4. To A_7 t_2+ (*navy+*) we glue A_8 and to A_8 t_2+ (*navy+*) we glue A_9 .

With these 9 tiles all we need for our exposition is in place. Our last action is the glueing of A_{10} to the edge t_2- (*navy-*) of A_2 . This action seems innocent enough but on closer examination, we see that A_{10} will zip-up with A_4 , A_6 and A_8 , which leaves A_9 in the same position as A_1 , since A_1 would actually match the already connected edge t_2+ (*navy+*) of A_8 . We thus arrive at an impasse. See figure 21.

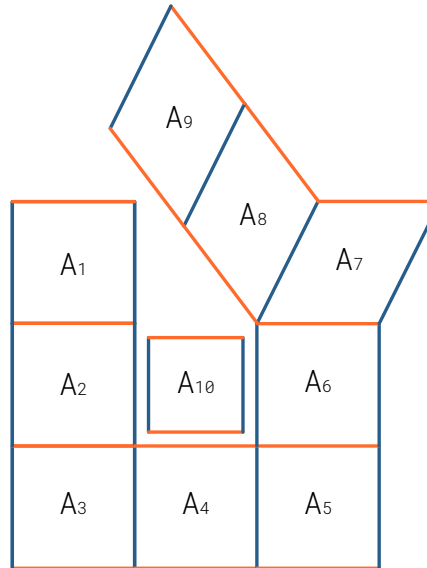
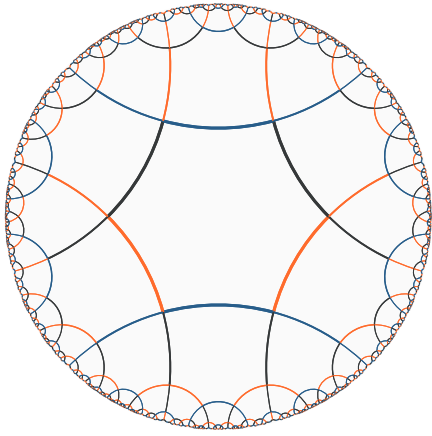


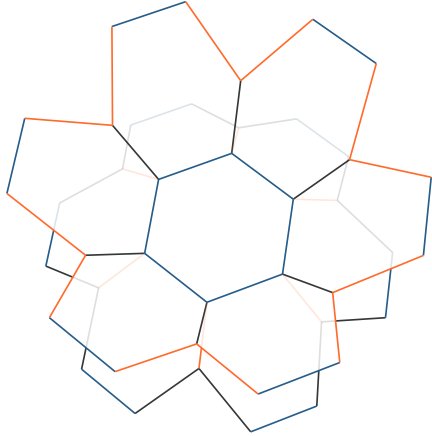
Figure 21: Invalid Induced Zip-Up

4.5.2 Single Neck {6,4}

This example demonstrates how certain seeds can be used to reach compositions otherwise not attainable. Table 9 tells us that complete edge-neighbourhoods of vertices in a tilegraph made up of base tiles of the n -colouring $t^2t^3t^2$ will always have an indegree of 4. Thus if we were to grow our tilegraph additively starting from one tile as described in section 2.5, without having defined any looping cycles, we would end up with a tilegraph that could be embedded in the hyperbolic plane as a 6,4 tiling (figure 22a).



(a) $\{6,4\}$ Tiling Hyperbolic Plane



(b) Seed of two Six-Tile Rings

Figure 22: Single Neck Growth

To make our case, we replace the single tile seed by a multi tile composition constructed in the following way.

Let $S = \{A_1, A_2, \dots, A_{12}\}$ be a set of twelve tiles of n-colouring $t^2t^3t^2$.

1. We create a first ring with 6 tiles each by consecutively glueing their tiles together via t_1- (*kaki-*).
2. We create a second ring with 6 tiles each by consecutively glueing their tiles together via t_1- (*onyx-*).
3. We combine the two rings by glueing the edge t_2- (*navy-*) of A_1 to t_2+ (*navy+*) of A_7 and letting the zip-up take care of the rest of the t_2 boundary.

We see (figure 22b) that we have created a hexagonal hole in the tilegraph and have two isomorphic boundaries if we ignore their different colouring. If we use the current tilegraph as a seed for our default growth process rather than a single tile, we see that we can grow it indefinitely from its boundary.

4.6 N-Colouring Index

Below you will find the complete n-colourings for $n \leq 7$. Only excerpts are given for the further n-colourings of up to 13 colours. For complete lists

please consult the files under <https://github.com/jorgens/Transpositional-Topology/tree/main/n-colourings>.

The following information is shown for every n-colouring:

n-Colouring The sequence of colours in the n-colouring

Index The unique index of the n-colouring

Signature The unique signature of the n-colouring

Gyre Count The number of different gyres in any resulting tilegraph

Face-Pivot Incidence The number of faces incident to any vertex of the n-colouring in the setting of complete edge-neighbourhoods of a tilegraph

Mirror The signature of the mirror n-colouring that can be obtained by inverting the direction of the n-colouring cycle. A * is used to indicate that a n-colouring is its own mirror n-colouring

For more on the meaning of the different fields have a look at sections 4.1.1 and 2.4.

4.7 N-Colouring Tables

n-Colouring	Index	Signature	Gyre Count	Face-Pivot Incidence	Mirror
f	1	f	-	-	*

Table 4: 1-colouring

n-Colouring	Index	Signature	Gyre Count	Face-Pivot Incidence	Mirror
t_1, t_1	11	t^1	2	[3, 3]	*
f, f	22	$2f$	1	[4, 4]	*

Table 5: 2-colourings and Gyres (All)

n-Colouring	Index	Signature	Gyre Count	Face-Pivot Incidence	Mirror
t_1, t_1, f	123	$t^1 f$	2	[3, 4, 4]	*
f, f, f	333	$3f$	1	[3, 3, 3]	*

Table 6: 3-colourings and Gyres (All)

n-Colouring	Index	Signature	Gyre Count	Face-Pivot Incidence	Mirror
t_1, t_1, t_2, t_2	1313	$2t^1$	3	[3, 4, 3, 4]	*
t_1, t_1, f, f	1344	$t^1 2f$	2	[3, 3, 3, 3]	*
t_1, t_2, t_1, t_2	2222	$2t^2$	1	[4, 4, 4, 4]	*
t_1, f, t_1, f	2424	$t^2 2f$	2	[4, 4, 4, 4]	*
f, f, f, f	4444	$4f$	1	[4, 4, 4, 4]	*

Table 7: 4-colourings and Gyres (All)

n-Colouring	Index	Signature	Gyre Count	Face-Pivot Incidence	Mirror
t_1, t_1, t_2, t_2, f	14145	$2t^1 f$	3	[3, 3, 3, 3, 3]	*
t_1, t_1, t_2, f, t_2	14253	$t^1 t^2 f$	3	[3, 4, 4, 4, 4]	*
t_1, t_1, f, f, f	14555	$t^1 3f$	2	[3, 4, 4, 4, 4]	*
t_1, t_2, t_1, t_2, f	22335	$2t^2 f$	1	[5, 5, 5, 5, 5]	*
t_1, f, t_1, f, f	25355	$t^2 3f$	2	[4, 4, 3, 3, 3]	*
f, f, f, f, f	55555	$5f$	1	[5, 5, 5, 5, 5]	*

Table 8: 5-colourings and Gyres (All)

n-Colouring	Index	Signature	Gyre Count	Face-Pivot Incidence	Mirror
$t_1, t_1, t_2, t_2, t_3, t_3$	151515	$3t^1$	4	[3, 3, 3, 3, 3, 3]	*
t_1, t_1, t_2, t_2, f, f	151566	$2t^1 2f$	3	[3, 4, 3, 4, 4, 4]	*
$t_1, t_1, t_2, t_3, t_2, t_3$	152244	$t^1 2t^2$	2	[3, 5, 5, 5, 5, 5]	*
t_1, t_1, t_2, f, t_2, f	152646	$t^1 t^2 2f$	3	[3, 3, 4, 4, 3, 3]	$t^1 f t^2 f$
$t_1, t_1, t_2, t_3, t_3, t_2$	153153	$t^1 t^3 t^1$	4	[3, 4, 4, 3, 4, 4]	*
t_1, t_1, t_2, f, f, t_2	153663	$t^1 t^3 2f$	3	[3, 4, 3, 3, 3, 4]	*
t_1, t_1, f, t_2, t_2, f	156156	$t^1 f t^1 f$	3	[3, 4, 4, 3, 4, 4]	*
t_1, t_1, f, t_2, f, t_2	156264	$t^1 f t^2 f$	3	[3, 3, 3, 4, 4, 3]	$t^1 t^2 2f$
t_1, t_1, f, f, f, f	156666	$t^1 4f$	2	[3, 5, 5, 5, 5, 5]	*
t_1, t_2, t_1, t_2, f, f	224466	$2t^2 2f$	1	[6, 6, 6, 6, 6, 6]	*
$t_1, t_2, t_1, t_3, t_2, t_3$	234234	$t^2 t^3 t^2$	2	[4, 4, 4, 4, 4, 4]	*
t_1, t_2, t_1, f, t_2, f	234636	$t^2 t^3 2f$	1	[6, 6, 6, 6, 6, 6]	*
t_1, f, t_1, t_2, f, t_2	264264	$t^2 f t^2 f$	3	[4, 4, 4, 4, 4, 4]	*
t_1, f, t_1, f, f, f	264666	$t^2 4f$	2	[4, 4, 4, 4, 4, 4]	*
$t_1, t_2, t_3, t_1, t_2, t_3$	333333	$3t^3$	2	[3, 3, 3, 3, 3, 3]	*
t_1, t_2, f, t_1, t_2, f	336336	$2t^3 2f$	1	[6, 6, 6, 6, 6, 6]	*
t_1, f, f, t_1, f, f	366366	$t^3 4f$	2	[3, 3, 3, 3, 3, 3]	*

f, f, f, f, f, f	666666	$6f$	1	[6, 6, 6, 6, 6, 6]	*
--------------------	--------	------	---	--------------------	---

Table 9: 6-colourings and Gyres (All)

n-Colouring	Index	Signature	Gyre Count	Face-Pivot Incidence	Mirror
$t1, t1, t2, t2, t3, t3, f$	1616167	$3t^1f$	4	[3, 4, 3, 4, 3, 4, 4]	*
$t1, t1, t2, t2, t3, f, t3$	1616275	$2t^1t^2f$	4	[3, 3, 3, 3, 4, 4, 3]	*
$t1, t1, t2, t2, f, f, f$	1616777	$2t^13f$	3	[3, 5, 3, 5, 5, 5, 5]	*
$t1, t1, t2, t3, t2, t3, f$	1622557	t^12t^2f	2	[3, 6, 6, 6, 6, 6]	t^1f2t^2
$t1, t1, t2, t3, t2, f, t3$	1623574	$t^1t^2t^3f$	2	[3, 6, 6, 6, 6, 6]	$t^1t^3ft^2$
$t1, t1, t2, f, t2, f, f$	1627577	t^1t^23f	3	[3, 4, 4, 4, 4, 4, 4]	t^12ft^2f
$t1, t1, t2, t3, t3, t2, f$	1631647	$t^1t^3t^1f$	4	[3, 3, 4, 3, 4, 3, 3]	$t^1t^4t^1f$
$t1, t1, t2, t3, f, t2, t3$	1633744	t^12t^3f	2	[3, 6, 6, 6, 6, 6]	*
$t1, t1, t2, f, t3, t2, t3$	1637245	$t^1t^3ft^2$	2	[3, 6, 6, 6, 6, 6]	$t^1t^2t^3f$
$t1, t1, t2, f, f, t2, f$	1637747	t^1t^33f	3	[3, 3, 3, 3, 3, 3, 3]	t^1ft^32f
$t1, t1, t2, t3, t3, f, t2$	1641673	$t^1t^4t^1f$	4	[3, 4, 3, 3, 3, 3, 4]	$t^1t^3t^1f$
$t1, t1, t2, t3, f, t3, t2$	1642753	$t^1t^4t^2f$	4	[3, 4, 4, 4, 4, 4, 4]	*
$t1, t1, t2, f, f, f, t2$	1647773	t^1t^43f	3	[3, 4, 4, 4, 4, 4, 4]	*
$t1, t1, f, t2, t2, f, f$	1671677	t^1ft^12f	3	[3, 5, 5, 3, 5, 5, 5]	*
$t1, t1, f, t2, t3, t2, t3$	1672255	t^1f2t^2	2	[3, 6, 6, 6, 6, 6]	t^12t^2f
$t1, t1, f, t2, f, t2, f$	1672757	t^1ft^22f	3	[3, 4, 4, 4, 4, 4, 4]	*
$t1, t1, f, t2, f, f, t2$	1673774	t^1ft^32f	3	[3, 3, 3, 3, 3, 3, 3]	t^1t^33f
$t1, t1, f, f, t2, f, t2$	1677275	t^12ft^2f	3	[3, 4, 4, 4, 4, 4, 4]	t^1t^32f
$t1, t1, f, f, f, f, f$	1677777	t^15f	2	[3, 6, 6, 6, 6, 6]	*
$t1, t2, t1, t2, t3, f, t3$	2255275	$3t^2f$	2	[5, 5, 5, 5, 4, 4, 5]	*
$t1, t2, t1, t2, f, f, f$	2255777	$2t^23f$	1	[7, 7, 7, 7, 7, 7, 7]	*
$t1, t2, t1, t3, t2, t3, f$	2352457	$t^2t^3t^2f$	2	[4, 4, 3, 4, 4, 3, 3]	*
$t1, t2, t1, t3, t2, f, t3$	2353474	t^22t^3f	2	[5, 5, 4, 5, 5, 5, 4]	$t^2t^4t^3f$
$t1, t2, t1, f, t2, f, f$	2357477	t^2t^33f	1	[7, 7, 7, 7, 7, 7, 7]	t^2t^43f
$t1, t2, t1, t3, f, t2, t3$	2453734	$t^2t^4t^3f$	2	[5, 5, 4, 5, 5, 5, 4]	$t^2t^3t^3f$
$t1, t2, t1, f, f, t2, f$	2457737	t^2t^43f	1	[7, 7, 7, 7, 7, 7, 7]	t^2t^33f
$t1, f, t1, t2, f, t2, f$	2752757	t^2ft^22f	3	[4, 4, 3, 4, 4, 3, 3]	*
$t1, f, t1, t2, f, f, t2$	2753774	t^2ft^32f	3	[4, 4, 4, 3, 3, 3, 4]	*
$t1, f, t1, f, f, f, f$	2757777	t^25f	2	[4, 4, 5, 5, 5, 5, 5]	*
$t1, t2, t3, t1, t2, t3, f$	3334447	$3t^3f$	2	[3, 4, 3, 4, 3, 4, 4]	*
$t1, t2, f, t1, t2, f, f$	3374477	$2t^33f$	1	[7, 7, 7, 7, 7, 7, 7]	*
$t1, t2, f, t1, f, t2, f$	3474737	t^3t^43f	1	[7, 7, 7, 7, 7, 7, 7]	*
$t1, f, f, t1, f, f, f$	3774777	t^35f	2	[3, 3, 3, 4, 4, 4, 4]	*
f, f, f, f, f, f, f	7777777	$7f$	1	[7, 7, 7, 7, 7, 7, 7]	*

Table 10: 7-colourings and Gyres (All)

n-Colouring	Index	Signature	Gyre Count	Face-Pivot Incidence	Mirror
$t1, t1, t2, t2, t3, t3, t4, t4$	17171717	$4t^1$	5	[3, 4, 3, 4, 3, 4, 3, 4]	*
$t1, t1, t2, t2, t3, t3, f, f$	17171788	$3t^12f$	4	[3, 5, 3, 5, 3, 5, 5, 5]	*
$t1, t1, t2, t2, t3, t4, t3, t4$	17172266	$2t^12t^2$	3	[3, 6, 3, 6, 6, 6, 6, 6]	*
$t1, t1, t2, t2, t3, f, t3, f$	17172868	$2t^1t^22f$	4	[3, 4, 3, 4, 4, 4, 4, 4]	$2t^1ft^2f$
$t1, t1, t2, t2, t3, t4, t4, t3$	17173175	$2t^1t^3t^1$	5	[3, 3, 3, 3, 4, 3, 4, 3]	*
$t1, t1, t2, t2, t3, f, f, t3$	17173885	$2t^1t^32f$	4	[3, 3, 3, 3, 3, 3, 3, 3]	*
$t1, t1, t2, t2, f, t3, t3, f$	17178178	$2t^1ft^1f$	4	[3, 5, 3, 5, 5, 3, 5, 5]	*
...

Table 11: 8-colourings and Gyres (7 of 108)

n-Colouring	Index	Signature	Gyre Count	Face-Pivot Incidence	Mirror
$t1, t1, t2, t2, t3, t3, t4, t4, f$	181818189	$4t^1f$	5	[3, 5, 3, 5, 3, 5, 3, 5]	*
$t1, t1, t2, t2, t3, t3, t4, f, t4$	181818297	$3t^1t^2f$	5	[3, 4, 3, 4, 3, 4, 4, 4]	*
$t1, t1, t2, t2, t3, t3, f, f, f$	181818999	$3t^13f$	4	[3, 6, 3, 6, 3, 6, 6, 6]	*

$t1, t1, t2, t2, t3, t4, t3, t4, f$	181822779	$2t^1 2t^2 f$	3	[3, 7, 3, 7, 7, 7, 7, 7]	$2t^1 f 2t^2$
$t1, t1, t2, t2, t3, t4, t3, f, t4$	181823796	$2t^1 t^2 t^3 f$	3	[3, 7, 3, 7, 7, 7, 7, 7]	$2t^1 t^3 f t^2$
$t1, t1, t2, t2, t3, f, t3, f, f$	181829799	$2t^1 t^2 3f$	4	[3, 5, 3, 5, 4, 4, 5, 5, 5]	$2t^1 2f t^2 f$
$t1, t1, t2, t2, t3, t4, t4, t3, f$	181831869	$2t^1 t^3 t^1 f$	5	[3, 4, 3, 4, 4, 3, 4, 4, 4]	$2t^1 f t^3 t^1$
...

Table 12: 9-colourings and Gyres (7 of 294)

n-Colouring	Index	Signature	Gyre Count	Face-Pivot Incidence	Mirror
$t1, t1, t2, t2, t3, t3, t4, t4, t5, t5$	10901090109010901090109	$5t^1$	6	[3, 5, 3, 5, 3, 5, 3, 5, 3, 5]	*
$t1, t1, t2, t2, t3, t3, t4, t4, f, f$	10901090109010901090109	$4t^1 2f$	5	[3, 6, 3, 6, 3, 6, 3, 6, 6, 6]	*
$t1, t1, t2, t2, t3, t3, t4, t5, t4, t5$	1090109010902020808	$3t^1 2t^2$	4	[3, 7, 3, 7, 3, 7, 7, 7, 7]	*
$t1, t1, t2, t2, t3, t3, t4, t4, f, t4, f$	1090109010902100810	$3t^1 t^2 2f$	5	[3, 5, 3, 5, 3, 5, 4, 4, 5, 5]	$3t^1 f t^2 f$
$t1, t1, t2, t2, t3, t3, t4, t5, t5, t4$	1090109010903010907	$3t^1 t^3 t^1$	6	[3, 4, 3, 4, 3, 4, 4, 3, 4, 4]	*
$t1, t1, t2, t2, t3, t3, t4, f, f, t4$	1090109010903101007	$3t^1 t^3 2f$	5	[3, 4, 3, 4, 3, 4, 3, 3, 3, 4]	*
$t1, t1, t2, t2, t3, t3, f, t4, t4, f$	1090109010910010910	$3t^1 f t^1 f$	5	[3, 6, 3, 6, 3, 6, 3, 6, 6]	*
...

Table 13: 10-colourings and Gyres (7 of 984)

n-Colouring	Index	Signature	Gyre Count	Face-Pivot Incidence	Mirror
$t1, t1, t2, t2, t3, t3, t4, t4, t5, t5, f$	1100110011001100110011011	$5t^1 f$	6	[3, 6, 3, 6, 3, 6, 3, 6, 6, 6]	*
$t1, t1, t2, t2, t3, t3, t4, t4, t5, f, t5$	110011001100110021109	$4t^1 t^2 f$	6	[3, 5, 3, 5, 3, 5, 3, 5, 4, 4, 5]	*
$t1, t1, t2, t2, t3, t3, t4, t4, f, f, f$	1100110011001101111111	$4t^1 3f$	5	[3, 7, 3, 7, 3, 7, 3, 7, 7, 7]	*
$t1, t1, t2, t2, t3, t3, t4, t4, t5, t4, t5, f$	110011001100202090911	$3t^1 2t^2 f$	4	[3, 8, 3, 8, 3, 8, 8, 8, 8, 8, 8]	$3t^1 f 2t^2$
$t1, t1, t2, t2, t3, t3, t4, t4, t5, t4, t5, f, t5$	110011001100203091108	$3t^1 t^2 t^3 f$	4	[3, 8, 3, 8, 3, 8, 8, 8, 8, 8, 8]	$3t^1 t^3 f t^2$
$t1, t1, t2, t2, t3, t3, t4, f, t4, f, f$	110011001100211091111	$3t^1 t^2 3f$	5	[3, 6, 3, 6, 3, 6, 4, 4, 6, 6, 6]	$3t^1 2f t^2 f$
$t1, t1, t2, t2, t3, t3, t4, t4, t5, t5, t4, f$	110011001100301100811	$3t^1 t^3 t^1 f$	6	[3, 5, 3, 5, 3, 5, 4, 3, 4, 5, 5]	$3t^1 f t^3 t^1$
...

Table 14: 11-colourings and Gyres (7 of 3246)

n-Colouring	Index	Signature	Gyre Count	Face-Pivot Incidence	Mirror
$t1, t1, t2, t2, t3, t3, t4, t4, t5, t5, t6, t6$	11101110111011101110111011	$6t^1$	7	[3, 6, 3, 6, 3, 6, 3, 6, 3, 6]	*
$t1, t1, t2, t2, t3, t3, t4, t4, t5, t5, f, f$	11101110111011101110111212	$5t^1 2f$	6	[3, 7, 3, 7, 3, 7, 3, 7, 3, 7, 7]	*
$t1, t1, t2, t2, t3, t3, t4, t4, t5, t6, t5, t6$	11101110111011102021010	$4t^1 2t^2$	5	[3, 8, 3, 8, 3, 8, 3, 8, 8, 8, 8]	*
$t1, t1, t2, t2, t3, t3, t4, t4, t5, t5, f, t5, f$	11101110111011102121012	$4t^1 t^2 2f$	6	[3, 6, 3, 6, 3, 6, 4, 4, 6, 6]	$4t^1 f t^2 f$
$t1, t1, t2, t2, t3, t3, t4, t4, t5, t6, t6, t5$	11101110111011103011109	$4t^1 t^3 t^1$	7	[3, 5, 3, 5, 3, 5, 3, 5, 4, 3, 5]	*
$t1, t1, t2, t2, t3, t3, t4, t4, t5, f, f, t5$	11101110111011103121209	$4t^1 t^3 2f$	6	[3, 5, 3, 5, 3, 5, 3, 5, 3, 3, 5]	*
$t1, t1, t2, t2, t3, t3, t4, t4, f, t5, t5, f$	11101110111011112011112	$4t^1 f t^1 f$	6	[3, 7, 3, 7, 3, 7, 3, 7, 3, 7]	*
...

Table 15: 12-colourings and Gyres (7 of 11810)

n-Colouring	Index	Signature	Gyre Count	Face-Pivot Incidence	Mirror
$t1, t1, t2, t2, t3, t3, t4, t4, t5, t5, t6, t6, f$	1120112011201120112011213	$6t^1 f$	7	[3, 7, 3, 7, 3, 7, 3, 7, 3, 7, 7]	*
$t1, t1, t2, t2, t3, t3, t4, t4, t5, t5, t6, f, f$	1120112011201120112021311	$5t^1 t^2 f$	7	[3, 6, 3, 6, 3, 6, 3, 6, 3, 6, 4, 4, 6]	*
$t1, t1, t2, t2, t3, t3, t4, t4, t5, t5, f, f, f$	11201120112011201121313	$5t^1 3f$	6	[3, 8, 3, 8, 3, 8, 3, 8, 8, 8, 8]	*
$t1, t1, t2, t2, t3, t3, t4, t4, t5, t6, t5, t6, f$	11201120112011202111113	$4t^1 2t^2 f$	5	[3, 9, 3, 9, 3, 9, 3, 9, 9, 9, 9, 9]	$4t^1 f 2t^2$
$t1, t1, t2, t2, t3, t3, t4, t4, t5, t6, t5, f, t6, f$	1120112011201120203111310	$4t^1 t^2 t^3 f$	5	[3, 9, 3, 9, 3, 9, 3, 9, 9, 9, 9, 9]	$4t^1 t^3 f t^2$
$t1, t1, t2, t2, t3, t3, t4, t4, t5, f, t5, f, t5, f$	1120112011201120213111313	$4t^1 t^2 3f$	6	[3, 7, 3, 7, 3, 7, 3, 7, 4, 4, 7, 7]	$4t^1 2f t^2 f$
$t1, t1, t2, t2, t3, t3, t4, t4, t5, t6, t6, t5, f, t5, f$	1120112011201120301121013	$4t^1 t^3 t^1 f$	7	[3, 6, 3, 6, 3, 6, 4, 3, 4, 6, 6]	$4t^1 f t^3 t^1$
...

Table 16: 13-colourings and Gyres (7 of 43732)

4.8 Colour Coding

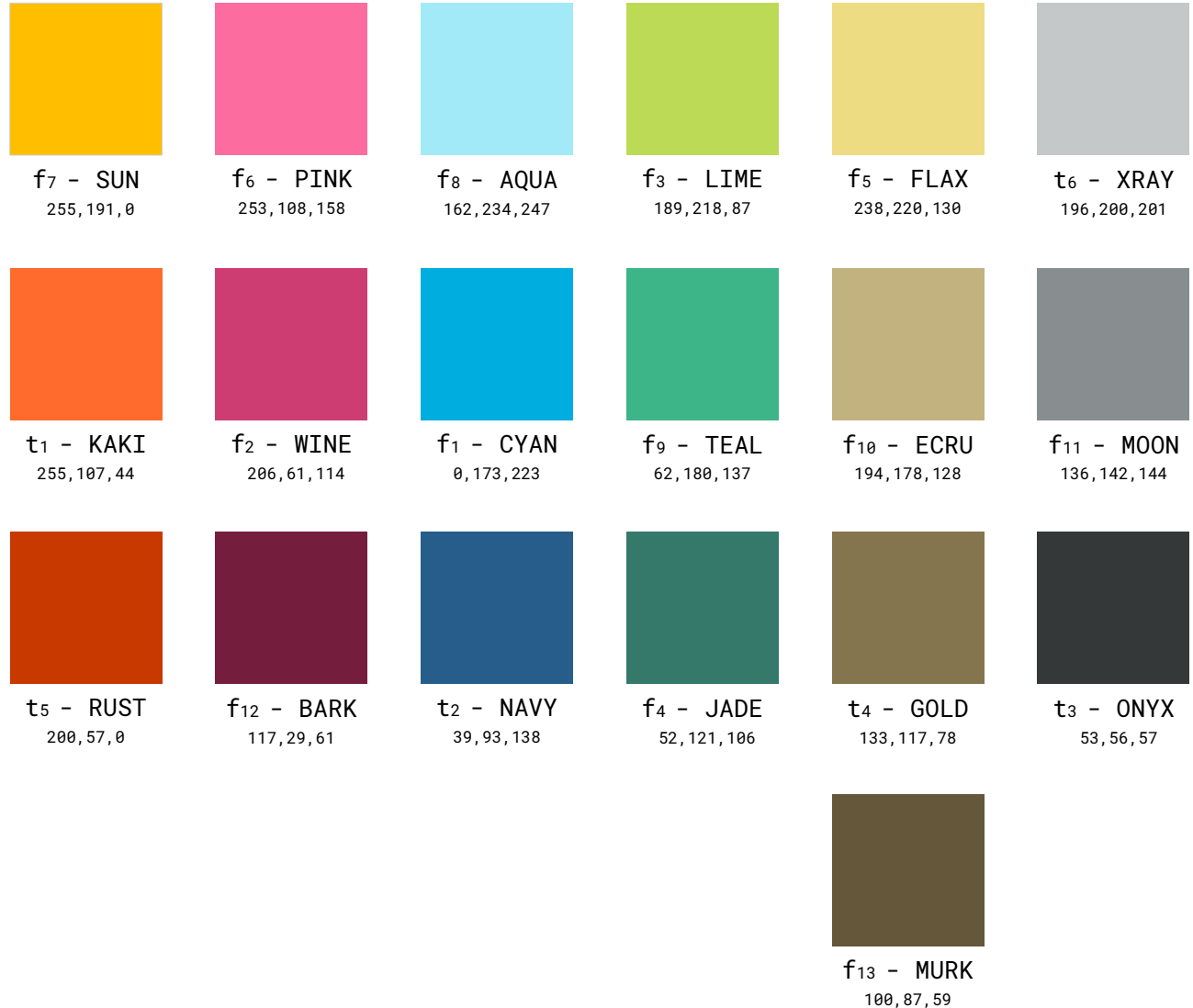


Figure 23: Colour coding of diagrams for n-colourings with $1 \leq n \leq 13$ organized by hue

References

- [1] Mario Botsch et al. *Polygon Mesh Processing*. Boca Raton, Fla: CRC Press, 2010. ISBN: 978-1-568-81426-1.
- [2] H. S. M. Coxeter. “Regular Skew Polyhedra in Three and Four Dimension, and their Topological Analogues”. In: *Proceedings of the London Mathematical Society* s2-43.1 (1938), pp. 33–62. DOI: 10.1112/plms/s2-43.1.33. URL: <https://doi.org/10.1112/plms/s2-43.1.33>.
- [3] H.S.M. Coxeter. *Regular Polytopes*. Dover books on advanced mathematics. Dover Publications, 1973, pp. 292–293. ISBN: 9780486614809. URL: <https://books.google.ch/books?id=iWvXsVIInpgMC>.
- [4] Erik Garrison. *multipermute*. Tech. rep. Version master. Dec. 21, 2020. URL: <https://github.com/ekg/multipermute>.
- [5] Aric Hagberg, Pieter Swart, and Daniel S Chult. *Exploring network structure, dynamics, and function using NetworkX*. Tech. rep. Los Alamos National Lab.(LANL), Los Alamos, NM (United States), 2008.
- [6] Tomihisa Kamada and Satoru Kawai. “An algorithm for drawing general undirected graphs”. In: *Information Processing Letters* 31.1 (Apr. 1989), pp. 7–15. DOI: 10.1016/0020-0190(89)90102-6. URL: [https://doi.org/10.1016/0020-0190\(89\)90102-6](https://doi.org/10.1016/0020-0190(89)90102-6).
- [7] Brendan D. McKay and Adolfo Piperno. “Practical graph isomorphism, II”. In: *Journal of Symbolic Computation* 60 (Jan. 2014), pp. 94–112. DOI: 10.1016/j.jsc.2013.09.003. URL: <https://doi.org/10.1016/j.jsc.2013.09.003>.
- [8] Alan H. Schoen. “Infinite Periodic Minimal Surfaces”. In: (May 1970). URL: [https://schoengeometry.com/e-tpms-media/19700020472_1970020472\[1\].pdf](https://schoengeometry.com/e-tpms-media/19700020472_1970020472[1].pdf).
- [9] Paul Steinhardt. *The Second Kind of Impossible - The Extraordinary Quest for a New Form of Matter*. New York: Simon and Schuster, 2019. ISBN: 978-1-476-72994-7.
- [10] Richard J Trudeau. *Introduction to graph theory*. en. 2nd ed. Mineola, NY: Dover Publications, 1994.
- [11] Aaron Williams. *Loopless generation of multi-set permutations using a constant number of variables by prefix shifts*. Ed. by Claire Mathieu. SIAM, 2009, pp. 987–996. URL: <http://dl.acm.org/citation.cfm?id=1496770.1496877>.